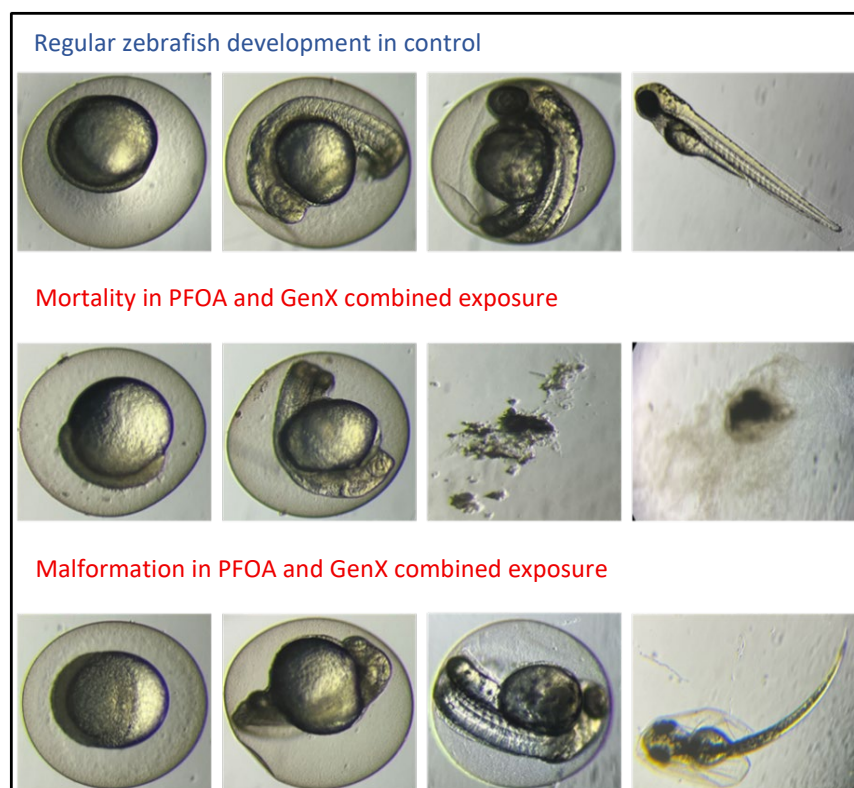


July 2025

COLLECTIVE EFFECTS OF DIFFERENT PER- AND POLYFLUOROALKYL SUBSTANCES (PFAS) CHEMICALS ON MIGRATION BEHAVIORS AND TOXICITY

NM WRI Technical Completion Report No. 410

**Runwei Li
Yanyan Zhang
Lin Wang
Yun Ma
Dulith Rajapakshe**



Zebrafish embryo development under PFOA and GenX combined exposure.

New Mexico Water Resources Research Institute
New Mexico State University
MSC 3167, P.O. Box 30001
Las Cruces, New Mexico 88003-0001
(575) 646-4337 email: nmwrri@nmsu.edu



**COLLECTIVE EFFECTS OF DIFFERENT PER- AND POLYFLUOROALKYL
SUBSTANCES (PFAS) CHEMICALS ON MIGRATION BEHAVIORS AND TOXICITY**

By

Runwei Li, Ph.D., Assistant Professor
Yanyan Zhang, Ph.D., Associate Professor
Lin Wang, Research Assistant
Yun Ma, Research Assistant
Dulith Rajapakshe, Research Assistant

Department of Civil Engineering
College of Engineering
New Mexico State University

TECHNICAL COMPLETION REPORT
Account Number 136707
Technical Completion Report #410

July 2025

The research on which this report is based was financed in part by the U.S. Department of the Interior, Geological Survey, through the New Mexico Water Resources Research Institute. This material is based upon work supported by the U.S. Geological Survey under Grant/Cooperative Agreement No. (G21AP10635).

Page Intentionally Left Blank

DISCLAIMER

The purpose of the NM Water Resources Research Institute (NM WRRI) technical reports is to provide a timely outlet for research results obtained on projects supported in whole or in part by the institute. Through these reports the NM WRRI promotes the free exchange of information and ideas and hopes to stimulate thoughtful discussions and actions that may lead to resolution of water problems. The NM WRRI, through peer review of draft reports, attempts to substantiate the accuracy of information contained within its reports, but the views and conclusions contained in this document are those of the authors and should not be interpreted as representing the opinions or policies of the U.S. Geological Survey. Mention of trade names or commercial products does not constitute their endorsement by the U.S. Geological Survey.

ACKNOWLEDGEMENTS

We appreciate the financial support from the U.S. Geological Survey Water Resources Research Act 104b grant through the New Mexico Water Resources Research Institute. We also want to thank the following people for their contribution to this research project. William Bahureksa, Ph.D., NMSU postdoctoral researcher with the Research Core Program provided excellent technical support and analytical guidance on LC-MS characterization. Marco Cortez, M.S., Department of Civil Engineering, NMSU, assisted in the literature review analysis. Santiago Archuleta, B.S., Department of Civil Engineering, NMSU, helped with the experimental set-up and laboratory management.

ABSTRACT

Per- and polyfluoroalkyl substances (PFAS) are synthetic organofluorine chemicals that have been widely used in commercial products and industrial processes. Their ubiquitous occurrence, environmental persistence, and potential toxicity pose threats to the public and ecosystems. Due to the regulation on traditional long-chain PFAS, industrial applications of PFAS have shifted to novel short-chain PFAS. The simultaneous occurrence of traditional novel PFAS compounds leads to their co-transport in the subsurface and subsequent co-exposure to humans and wildlife. However, most previous studies applied unrealistic experimental conditions of single PFAS. Therefore, understanding may vary as to the real-world scenarios of co-occurrence. To better understand the migration of PFAS and their potential health risks, it is important to consider their collective effects during the investigation.

We investigated the collective effects of PFAS compounds with three proposed objectives, namely (1) summarizing PFAS co-occurrence, (2) investigating PFAS co-transport in the subsurface, and (3) studying toxicity due to PFAS co-exposure. Regarding the first objective, the occurrence of conventional long-chain PFAS and their novel alternatives in surface water and groundwater has been reviewed and summarized in this report. The review indicated a higher level of occurrence of PFAS in surface water than in groundwater. Our review also suggests that limited occurrences of novel PFAS substances have been identified to date. To address the second objective, the individual transport and co-transport of representative PFAS (i.e., PFOS and 6:2 Cl-PFESA) have been investigated via column experiments in silicon sand and subsequent breakthrough curve (BTC) simulations. Experimental observation indicated retardation of both conventional and novel PFAS compounds. More importantly, the transport of the PFAS alternative (i.e., 6:2 Cl-PFESA) is significantly enhanced by the PFAS co-occurrence. To address the third objective, the acute and chronic toxicity of PFAS co-exposure (i.e., PFOA and GenX) were investigated by *in vivo* experiments using zebrafish (*Danio rerio*). The observed toxicity in acute exposure is PFAS-dependent, with embryo death observed at different concentration ranges for PFOA, GenX, and co-exposure. Future studies with larger sample sizes are needed to confirm the trend. Moreover, we found that PFAS liver impacts increased with exposure levels, as evidenced by the concentration-dependent upregulation of selected genes.

Keywords: PFAS, Fate-and-transport, Exposure, Ecotoxicity

TABLE OF CONTENTS

DISCLAIMER	iii
ACKNOWLEDGEMENTS	iv
ABSTRACT.....	v
LIST OF FIGURES	vii
LIST OF TABLES	vii
LIST OF ABBREVIATIONS	vii
1 INTRODUCTION.....	1
1.1 Background.....	1
1.2 Knowledge Gaps and Motivation.....	2
1.3 Objectives	3
2 MATERIALS AND METHODOLOGY.....	3
2.1 Review Method	3
2.2 Column Experiments	4
2.3 Breakthrough Curves Simulation	5
2.4 Zebrafish Husbandry	6
2.5 Acute Toxicity Test	7
2.6 Chronic Co-Exposure Tests.....	8
2.7 Ethical Considerations.....	10
3 RESULTS AND DISCUSSION	11
3.1 PFAS Occurrence Review	11
3.2 PFAS Co-Transport	12
3.3 Acute Toxicity	15
3.4 Chronic Toxicity.....	19
3.5 Discussion.....	21
4 CONCLUSIONS	23
5 REFERENCES.....	24
6 APPENDICES	A1–A12

LIST OF FIGURES

Figure 1. Zebrafish housing system	7
Figure 2. Tracer BTC and model fitting	12
Figure 3. Individual transport BTCs and model fitting for (a) PFOS, and (b) 6:2 Cl-PFESA	13
Figure 4. Co-transport BTCs and model fitting for PFOS and 6:2 Cl-PFESA	14
Figure 5. Mortality rate of zebrafish embryos exposed to (a) PFOA, (b) GenX, and (c) the combination of PFOA and GenX	16
Figure 6. Malformation rate of zebrafish embryos exposed to (a) PFOA, (b) GenX, and (c) the combination of PFOA and GenX	18
Figure 7. Zebrafish embryo development under combined exposure of PFOA and GenX.....	19
Figure 8. Effects of combined exposure to PFOA and GenX at different concentrations on the expression of (a) <i>cyp1a</i> and <i>il6</i> gene, and (b) <i>vtg</i> and <i>fapb10a</i> gene.....	20

LIST OF TABLES

Table 1. Specific primer sequences used in the qPCR experiments	10
Table 2. PFAS occurrence in groundwater (GW) and surface water (SW).....	12
Table 3. PFAS transport simulation results	15
Table 4. Apical observations of developmental delays in zebrafish embryos acutely exposed to PFOA, GenX, and their combination within 96 hours post-fertilization	19

LIST OF ABBREVIATIONS

Abbreviations	Full Names
BTC	Breakthrough curve
ddCT	Delta-Delta-CT
DI	Deionized
hpf	hours post-fertilization
IACUC	Institutional Animal Care and Use Committee
LC-MS	liquid chromatography-mass spectrometry
PFAS	Per- and polyfluoroalkyl substances
PFBS	Perfluorobutanesulfonic acid
PFHxS	Perfluorohexane sulfonate
PFNA	Perfluorononanoic acid
PFOA	Perfluorooctanoic acid
PFOS	Perfluorooctane sulfonic acid

Page Intentionally Left Blank

1 INTRODUCTION

1.1 Background

PFAS contamination currently is a significant emergent environmental problem. Since the invention of many PFAS compounds in the 1940s, they have been widely used in commercial products and industrial processes such as food packaging, water/oil-resistant materials, pesticides, and firefighting foams. PFAS are released to the environment during the manufacturing process and through the use and disposal of related consumer products. Over the past decades, PFAS have been detected in environmental samples worldwide, even in samples from remote regions such as Arctic and Alpine areas (Ahrens 2011; Brusseau et al. 2020; Goosey and Harrad 2012; Kirchgeorg et al. 2016). Their ubiquitous occurrence, environmental persistence, and potential toxicity pose threats to both the public and ecosystems. Although a series of long-chain PFAS, such as perfluorooctanoic acid (PFOA) and perfluorooctane sulfonic acid (PFOS), were phased out from production in the U.S., they are still applied internationally and enter the U.S. market via imported products. Moreover, even as some uses of PFOA and PFOS may have declined, short-chain PFAS, such as hexafluoropropylene oxide dimer acid (HFPO-DA, also known as GenX) and 6:2 chlorinated polyfluorinated ether sulfonate (6:2 Cl-PFESA, also known as the major part of F-53B), have been invented to replace the banned long-chain homologs and likely present similar environmental challenges. And novel short-chain alternatives are believed to have similar health impacts (Brendel et al. 2018). Recently, the U.S. EPA released a plan to establish a national primary drinking water regulation for the several following PFAS compounds: PFOA, PFOS, perfluorononanoic acid (PFNA), perfluorohexane sulfonate (PFHxS), perfluorobutanesulfonic acid (PFBS), and GenX (U.S. EPA 2024).

In New Mexico, the occurrence of PFAS pollution has also been reported. The application of firefighting foam at two Air Force Bases (i.e., Holloman and Cannon AFB) has been identified as the source for the PFAS occurrence in surrounding water resources. More recently, elevated concentrations of different PFAS have been detected in New Mexico groundwater from public and private wells in Curry, Otero, and Santa Fe Counties. These instances help demonstrate the urgent need for PFAS toxicity investigation and further action in New Mexico.

A significant body of growing literature indicates the association between PFAS exposure and a series of adverse health outcomes, such as increased risk of liver cancer, suppressed

immunity, and developmental toxicity problems (Dorts et al. 2011; Lee et al. 2017; Steenland and Winkler 2021; DeWitt et al. 2012; and Pelch et al. 2019). Recently, U.S. EPA released a plan to establish a national primary drinking water regulation for PFAS. Among these potentially regulated PFAS compounds, the newly proposed maximum contaminant levels values for PFOA and PFOS have been dramatically reduced from a combined health advisory previously of 70 ng/L now to 4 ng/L (U.S. EPA 2024). Locally, water scarcity in states like New Mexico motivates an even greater effort to understand the occurrence of PFAS and their subsequent migration.

1.2 Knowledge Gaps and Motivation

Previous researchers have expended significant effort to investigate the migration and toxicity of PFAS compounds. However, previous studies have often applied unrealistic experimental conditions including studying only the behavior of a single PFAS chemical at a time and also often only doing so at high concentrations. While such studies provide valuable information, these experimental conditions may not capture behavior under more realistic situations where co-occurrence of multiple PFAS compounds occurs. Our study targets using methodology to start to fill some of these types of knowledge gaps for both PFAS fate-and-transport and health risks aspects.

Co-transport of multiple PFAS compounds may be affected by both the chemistry of groundwater and the composition of solid media through which it flows (e.g., pH and types of adsorption sites) (Huang et al. 2018; Li et al. 2019a). These variables further complicate the understanding of the migration of PFAS compounds moving through porous media. Co-transport of multiple compounds likely alters the migration of some of those compounds.

The co-occurrence of multiple PFAS would also affect their potential health risks as the toxicity due to PFAS co-exposure may lead to worse health outcomes due to potential synergistic effects (Guo et al. 2009; Xin et al. 2023). Therefore, it is necessary to understand the collective effects of different PFAS compounds on their fate-and-transport behaviors, and potential health risks.

1.3 Objectives

In this project, three objectives were proposed to address the unknown collective effects of PFAS co-occurrence on their fate-and-transport and toxicity. Objective (1) was to derive the PFAS occurrence in surface water and groundwater via a systematic review. Objective (2) involved investigating PFAS co-transport in the subsurface using bench-scale sand column transport experiments and simulation of breakthrough curves. Objective (3) was to quantify the toxicity of PFAS co-exposure using zebrafish as an animal model in acute and chronic exposure experiments.

2 MATERIALS AND METHODOLOGY

2.1 Review Method

This study reviewed the occurrence of selected PFAS compounds dissolved in two different aqueous matrices, namely in surface water and groundwater. The PFAS concentrations through affected water bodies correspond to their mobility and represent their exposure risks to the public and ecosystems. The review method is adapted from our previous research (Li et al. 2019b).

For each matrix, we started the literature review by identifying and refining keywords to maximize our identification of pertinent articles. Three types of keywords were applied in this project including: (1) PFAS compounds full names, such as “perfluorooctanesulfonic acid” and “perfluorooctanoic acid”; (2) PFAS compounds short names, such as “PFOS” and “PFOA”; (3) matrix, such as “surface water” and “groundwater”; and (4) a characteristics description, such as “range,” “level,” and “concentration.” For each matrix, different combinations of keywords were used on two major academic search engines, namely, Web of Science and Google Scholar.

Publications returning from each search were first screened using their titles and abstracts. For example, a publication with the title “*Accumulation of PFOA and PFOS at the air–water interface*” was not selected in the review as the focus of this publication is the air-water interface rather than occurrence. In this initial step, publications in agreement with the review scope were recorded in terms of title and doi address. Then, our initial selection was further screened by reading through their full texts. Publications were excluded from the review due to at least one of the following reasons: (1) specific PFAS occurrence data is not reported in the full text, (2) PFAS

concentrations are reported with out-of-date quantification methods, and (3) PFAS occurrence data is reported in forms that are not quantitatively accessible (e.g., in a figure or map without specific numerical description).

After the screening step, the useful information related to PFAS occurrence was extracted from the full text and summarized in tables. Specific information extracted in the project included publication title, study location, related matrix, PFAS compounds, quantification methods, minimum concentration, maximum concentration, average concentration, number of observations, year of study, and potential source of PFAS contamination.

2.2 Column Experiments

Column experiments for individual and co-transport of PFAS were conducted using bench-scale acrylic columns with a length of 10 cm and an inner diameter of 1.1 cm. Commercially available sediment (Accusand®) was used as the porous media in our experiments. The sediment was first sieved to a size range of 0.3 to 0.5 μm to ensure homogeneity in the column. Sieved sediment was then cleaned with acid soaking and deionized (DI) water flushing to remove the potential surface organics. The porosity of pretreated sediment was characterized by estimating the water volume in a fully saturated condition. The design, preparation, and implementation of the column experiments followed methods we have used in previous research (Li et al. 2019a; Li et al. 2019c; Qi et al. 2022).

Specifically, the column was first wet packed with autoclaved and saturated sediments with the water table around 2 cm above the sediment top surface. The packed sediment column was flushed with DI water over night at a constant flow rate of 0.5 mL/min using a peristaltic pump. After DI water flushing, the column was subsequently flushed by LC-MS grade water for three pore volumes. The packing and flushing steps would guarantee the preparation of a stable column. All devices, including volumetric cylinders, glass beakers, acrylic columns, and fraction collector tubes, used in the experiments were pre-cleaned with LC-MS grade methanol and rinsed with LC-MS grade water to eliminate potential PFAS cross-contamination from surrounding environments.

Finally, three pore volumes of PFAS solution at a concentration of 200 $\mu\text{g/L}$ was injected into the column at the same flow rate of 0.5 mL/min. A fraction collector was used to receive

effluent at the other end of the column. For each pore volume, four aliquots of effluent were collected. The effluent samples were then filtered and characterized for PFAS concentrations with an LC-MS (Shimadzu 8050) using the EPA 1633 method (U.S. EPA 2021). The specific PFAS compounds selected in this study's co-transport experiments were PFOS and 6:2 Cl-PFESA, which is the major component of the PFOS alternative, F-53B. Both chemicals were purchased from Wellington Laboratories. The column experiments were run for three scenarios, including PFOS individual transport, 6:2 Cl-PFESA individual transport, and PFOS/6:2 Cl-PFESA co-transport. A conservative tracer column experiment was also performed at the same injection volume and flow rate to characterize unhindered flow parameters and to compare against potentially retarded PFAS transport.

Prior to performing PFAS and tracer transport experiments, a control experiment was performed with LC-MS grade water. Effluent samples from the control experiment were measured by the same analytical method and instrument. PFAS were not detected in control experiments, indicating a PFAS-free condition for subsequent column experiments.

2.3 Breakthrough Curves Simulation

CXTFIT 2.0, a nonlinear least-square optimization program (van Genuchten 1981), was used to solve the two-site advection dispersion transport model using parameters determined from the various experiments to match the non-reactive and reactive tracer data from the column experiments.

$$\beta R \frac{\partial C_1}{\partial T} = \frac{1}{p} \frac{\partial^2 C_1}{\partial Z^2} - \frac{\partial C_1}{\partial Z} - \omega(C_1 - C_2) - \mu_1 C_1 \quad (1)$$

$$(1 - \beta)R \frac{\partial C_2}{\partial T} = \omega(C_1 - C_2) - \mu_2 C_2 \quad (2)$$

where C_1 and C_2 are the dimensionless PFAS concentration in the solution and on the soil surface, respectively, β is the partition coefficient, ω is a dimensionless mass transfer coefficient, and R is the retardation factor ($R = 1 + \rho_b \frac{K_d}{\theta}$, where ρ_b is the media bulk density, K_d is the partition coefficient of between the solution and media, and θ is the porosity), T is the dimensionless time, P is the Peclet number ($P = \frac{vL}{D}$, where v is the interstitial pore-water velocity, L is the length of the

column, and D is the dispersion coefficient), and μ_1 and μ_2 are the dimensionless deposition coefficient in the solution and on the soil surface, respectively (Toride et al. 1995).

Specifically, the simulation was first conducted to fit the BTCs from tracer transport experiments. Assuming limited decay and retardation of tracer transport, the simulation only fitted the dispersion coefficient, which was further used as a constant input in the simulation of PFAS transport BTC. In addition, the retardation factor for each PFAS transport BTC was estimated from moment analysis and used as a constant input for the simulation. The numerical simulation of these physical fluid flow and reactive transport processes provides the link between observation and theory that tests our mechanistic conceptualization and prediction capabilities.

2.4 Zebrafish Husbandry

Zebrafish (*Danio rerio*) were selected for this study due to their widespread use in environmental toxicology studies (Li et al. 2019a). The fish were obtained from a certified supplier and maintained under standard laboratory conditions using a water-circulating system (Figure 1). Prior to the experiment, adult zebrafish were kept in a recirculating system at $27 \pm 1^\circ\text{C}$ with a 14-hour light/10-hour dark photoperiod. The fish were fed twice daily with commercially available zebrafish feed. Water quality parameters, including pH, dissolved oxygen, and temperature, were monitored daily to ensure optimal conditions. The pH was maintained between 7.0 and 8.0, dissolved oxygen levels were kept above 80% saturation, and ammonia and nitrite levels were kept below detectable limits. Solutions were renewed every 24 hours to maintain exposure concentrations and minimize degradation or microbial contamination. Fertilized fish embryos were collected within 4 hours post-fertilization (hpf) and used for the experiment. Only embryos at the blastula stage were selected for testing to ensure uniform developmental stages.

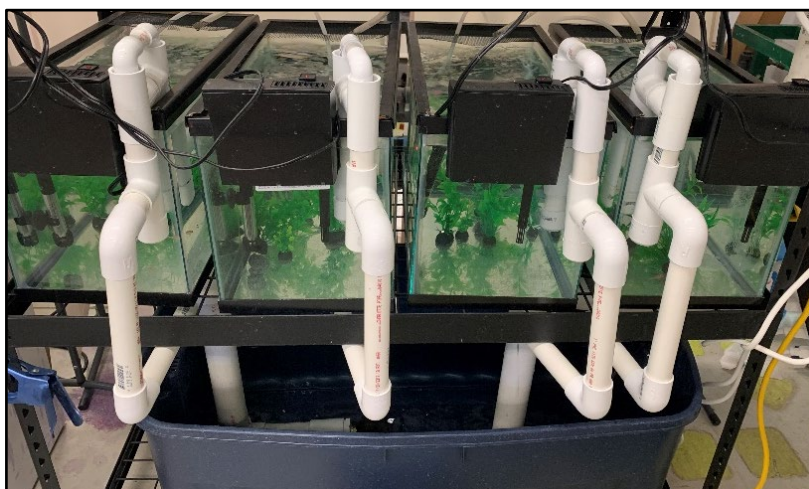


Figure 1. Zebrafish housing system

2.5 Acute Toxicity Test

The study followed the guidelines outlined in the OECD Test No. 236: Fish Embryo Acute Toxicity (FET) Test (OECD 2013). Specific PFAS selected in co-exposure experiments were PFOA and hexafluoropropylene oxide dimer acid GenX. Both chemicals were purchased from Wellington Laboratories. The experiment used embryos in four groups, including a control group, a PFOA individual exposure group, a GenX individual exposure group, and a PFOA/GenX co-exposure group. For each group, five concentrations were tested: 0.1 µg/L, 1 µg/L, 20 µg/L, 100 µg/L, and 200 µg/L. In the co-exposure group, the concentration of PFOA and GenX were set at a 1:1 ratio. Each concentration was applied to 24 embryos.

Under each exposure experiment, zebrafish embryos were placed individually into 24-well plates, with each well containing 3 mL of prepared PFAS exposure solution. The plates were covered to prevent evaporation and cross-contamination and then incubated at $27 \pm 1^\circ\text{C}$ under static conditions. The embryos were observed at 6 hpf, 24 hpf, 48 hpf, 72 hpf, and 96 hpf for mortality, malformation (including malformations such as spinal curvature, heart edema, and abnormal pigmentation), and developmental delay. Dead embryos were removed immediately to prevent contamination upon observation.

The assessment of endpoints in this study was conducted in accordance with the OECD 236 guidelines, ensuring a comprehensive evaluation of the effects of PFOA, GenX, and their combined exposure on zebrafish embryos. Several critical endpoints were systematically recorded throughout the exposure period, providing insight into the potential toxic effects of these substances.

Mortality was closely monitored at specific time points: 6 hpf, 24 hpf, 48 hpf, 72 hpf, and 96 hpf. The criteria for determining mortality included observable indicators such as coagulation of the embryo, lack of somite (transient structures) formation, failure of the tail to detach from the yolk sac, and the absence of a detectable heartbeat. Embryos displaying any of these signs were classified as dead, and the data were recorded accordingly to assess the lethality of the chemical exposures over time. The malformation rate was another crucial endpoint, with malformations being recorded at 24 hpf, 48 hpf, 72 hpf, and 96 hpf. Malformations observed included spinal curvature, heart edema, and abnormal pigmentation, all of which are indicative of developmental disruptions. These abnormalities were identified as any visible deviation from the normal embryonic development, and the rate of malformation provided a key measure of the sublethal effects of the exposures. Delayed development was specifically assessed at the 96-hour mark to evaluate the impact of PFOA, GenX, and their combined exposure on the timing of key developmental processes. Embryos that exhibited slower development compared to controls, such as delayed hatching, incomplete organ formation, or failure to reach the expected developmental milestones by 96 hpf, were recorded as displaying delayed development. This endpoint is crucial for understanding how chemical exposure can disrupt the normal developmental timeline, potentially leading to long-term consequences for the organism's health and survival.

2.6 Chronic Co-Exposure Tests

The collective effects were further investigated under long-term exposure experiments, with the liver selected as the representative organ. Female zebrafish were randomly divided into four co-exposure groups, including a control group, a 0.2 µg/L group, a 20 µg/L group, and a 200 µg/L group. Each group consisted of 15 fish, with 5 fish placed in each of three 2 L glass beakers to avoid tank effects. Throughout the 90-day period, the fish were continuously exposed to the PFOA and GenX mixtures. Every 24 hours, half of the solution in each beaker was replaced to maintain stable exposure concentrations and minimize chemical degradation. Water quality parameters, including pH, temperature, and dissolved oxygen, were monitored daily to ensure optimal living conditions for the fish during the experiment. At the end of the 90-day exposure period, fish were anesthetized using 125 mg/L MS-222 (tricaine methane sulfonate). The liver was quickly removed and placed in

RNAlater® solution to preserve RNA integrity, and all samples were stored at -80°C until RNA extraction.

To extract RNA using the Pure Link® RNA Mini Kit, the frozen tissue was first quickly thawed and handled on ice to prevent RNA degradation. An appropriate volume of lysis buffer, typically 1 mL per 50 mg of tissue, was used to ensure efficient lysis. The liver tissue and lysis buffer, which includes 2-mercaptoethanol, were placed into an RNase-free tube and homogenized thoroughly using a homogenizer to release RNA. After homogenization, the mixture was centrifuged to remove unlysed tissue. The clear supernatant was carefully transferred to a new RNase-free tube, applied to an RNA binding column, and centrifuged to bind the RNA to the column. The column was then washed with a buffer to eliminate non-RNA components. Finally, RNA was eluted from the column using a small volume of RNase-free water. The RNA's concentration and purity were assessed using a spectrophotometer to ensure suitability for further experimental analyses.

The RNA was then used to reverse transcribe cDNA. Before initiating cDNA preparation, DNase I treatment was applied to all RNA samples to eliminate any comingled DNA. The samples were gently mixed and then incubated at room temperature for 15 minutes. Subsequently, 1 µL of 25 mM EDTA solution was added to inactivate the DNase I, followed by heating the RNA sample at 65°C for 10 minutes, rendering it ready for reverse transcription. First-strand cDNA synthesis involved preparing the RNA template by adding specific reagents in a sterile, nuclease-free environment. After the thawing of reagents and briefly centrifuging the components, 1 µg of RNA was combined with 19 µL of reagents. The reaction was then incubated at 42°C for 60 minutes and terminated by heating at 70°C for 5 minutes.

Four specific genes were selected as indicators of liver activity and condition (Table 1). For each gene's primer, a stock solution of 100 mM was prepared by dissolving the lyophilized solids in water and vortexing gently. The working primer solutions (10 mM) were generated by performing a 10-fold dilution of the 100 mM stocks.

A master mix was prepared for the qPCR using the SsoAdvanced™ Universal SYBR® Green Supermix. Each qPCR reaction was assembled by adding 1 µL of primers to the master mix. Subsequently, 18 µL of primer-containing master mix was added to each well of a qPCR plate, followed by 2 µL of cDNA. The qPCR plate was then sealed with a microseal B adhesive sealer and

placed in the Real-Time System-CFX Connect. The qPCR protocol included an initial DNA denaturation at 95°C for 30 seconds, followed by a repeated denaturation at 95°C for 15 seconds, annealing/extension at 60°C for 15 seconds, and fluorescence reading at the same temperature, repeated across 35-40 cycles. Gene expression was quantified using the ddCT (Delta-Delta-CT) method, with fold changes calculated and normalized relative to control values from zebrafish tissues in the absence of endocrine disruptors.

Table 1. Specific primer sequences used in the qPCR experiments

Gene	Forward primer sequence (5'--3')	Reverse primer sequence (3'--5')	Reference
<i>cyp1a</i>	TTCACGCCATCACTGCCACA	TCAGGGATGACCTTGCCAACAG	25
<i>il6</i>	CCATCTTCTTCATCAGGGACGC	GGGTTTGAGGGTTTCGCTTCT	26
<i>vtg1</i>	TGCTCGCCATCAATCCCAGG	AAGCACCGTAGGACTCGTTCAG	27
<i>fabp10a</i>	CCTCGCTGAAGATTTTGTCC	TGTTGAAGCGGTTGTTGAGG	28

2.7 Ethical Considerations

All procedures involving animals were conducted in accordance with institutional and national guidelines for the care and use of laboratory animals. The study protocol was approved by the Institutional Animal Care and Use Committee (IACUC) of New Mexico State University, ensuring that all efforts were made to minimize animal suffering and reduce the number of animals used in the study. Additionally, the experimental design was carefully planned to adhere to the principles of the 3Rs (Replacement, Reduction, and Refinement) to ensure ethical and humane treatment of the zebrafish embryos. This detailed methodology ensures that the study results are robust, reproducible, and aligned with international standards for environmental toxicology research while also maintaining a high standard of animal welfare as mandated by New Mexico State University and relevant regulatory bodies.

3 RESULTS AND DISCUSSION

3.1 PFAS Occurrence Review

Four specific PFAS compounds were selected as the representatives in this project, including two conventional long-chain PFAS, namely PFOA and PFOS, and two novel alternatives, namely GenX and 6:2 Cl-PFESA. In total 36 publications with over 100 PFAS occurrence records over the world were selected in this review.

A summary of PFAS occurrences is included in Table 2. The 6:2 Cl-PFESA records were excluded from the table due to the limited records obtained from the screening process. According to our review, PFAS occurrence depends significantly on the matrix. For all reviewed compounds, surface water demonstrates higher minimum, maximum, and average concentrations as compared with groundwater. Widespread discharge of PFAS from various sources into surface water systems is obvious in the literature (Podder et al. 2021; Bai and Son 2021; Munoz et al. 2017). In addition, the two traditional PFAS have comparably elevated occurrence levels in surface water, which are significantly higher than their novel alternatives, suggesting that ongoing introduction of these traditional PFAS continues to be significant despite regulatory efforts to eliminate PFOA and PFOS.

It is important to mention that most PFAS records in this specific review were located in Asian countries, where PFAS have not been fully phased out from manufacturing processes, and therefore are more likely to have a higher level of PFAS occurrence. It is also noticed that most sampling locations are around large bodies of water such as rivers and lakes. This is suggestive of discharge from manufacturing factories. The awareness of these long-lasting contaminants' harmful effects on humans is prevalent in Asia's focus on sampling and studying these PFAS compounds and alternatives in the environment.

The detailed review data, including publication title, study location, related matrix, PFAS compounds, quantification methods, minimum concentration, maximum concentration, average concentration, number of observations, year of study, and potential source of PFAS contamination, are presented in the Appendices.

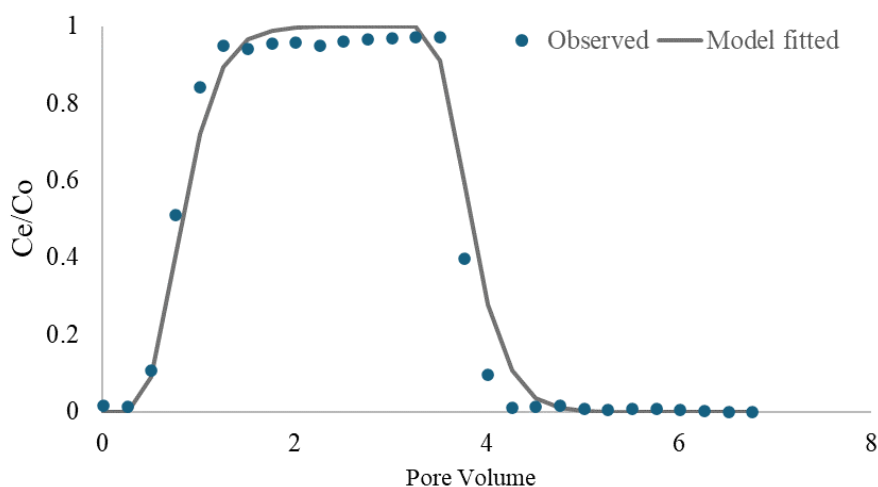
Table 2. PFAS occurrence in groundwater (GW) and surface water (SW) from literature review

Concentration	PFOA		PFOS		GenX	
	GW	SW	GW	SW	GW	SW
Minimum, ppt	0.04	0.2	0.0075	0.76	N/A	0.028
Average, ppt	1	3.26	0.21	4.26	N/A	0.684
Maximum, ppt	2	12	0.38	7.33	N/A	1.74

3.2 PFAS Co-Transport

In this project, chloride (from NaCl) was used as a tracer and the corresponding column experiment was conducted before introducing PFAS. The tracer was assumed to have no retardation in the column and the breakthrough curve would be only controlled by the flow parameters of the column run. In a realistic experimental run, the selected tracer has a retardation factor of around 1.1 with a retardation factor of 1 meaning no retardation. The tracer recovery was 97.2%. However, the potential adsorption of chloride by the sediment might occur in the column, which would skew the chloride BTC and therefore slightly increase the retardation factor from the ideal case (Figure 2).

In the simulation of the tracer BTC, the applied model achieved a fit with a coefficient of determination (R^2) of 0.975. The model appears to fit the initial front of the BTC very well but slightly deviates from the experimental results during the tailing part (Figure 2). The dispersion coefficient was estimated as 7.91 cm²/hour and was used as a fixed input constant for later PFAS simulations.

**Figure 2.** Tracer BTC and model fitting

After the tracer transport, the individual transport of PFOS and 6:2 Cl-PFESA were reviewed (Figure 3). Both PFOS and 6:2 Cl-PFESA transport in the sediment column was retarded when compared against the tracer and was characterized by their asymmetric BTCs. The recovery rates for PFOS and 6:2 Cl-PFESA individual transport were 86% and 81%, respectively (Table 3). Compared to PFOS transport, 6:2 Cl-PFESA BTC has a lower plateau and reaches the plateau $\frac{1}{4}$ pore volume later than PFOS. In addition, the 6:2 Cl-PFESA BTC has a longer tailing, which still elutes out of the sediment column at the pore volume of 7 (Figure 3). The observations suggested that both PFOS and 6:2 Cl-PFESA transport were subjected to the kinetic adsorption process, while 6:2 Cl-PFESA transport was also delayed more as compared to PFOS transport.

The experimental observations are supported by simulation outcomes. The retardation factor for 6:2 Cl-PFESA individual transport is 2.1, which is around 30% higher than that of PFOS individual transport. Moreover, the 6:2 Cl-PFESA BTC fitting has the highest mass transfer coefficient of 7.9×10^{-2} and the lowest partitioning coefficient of 0.843, indicating a higher fraction of kinetic sorption for 6:2 Cl-PFESA transport. All simulations achieved a good fitting performance with R^2 above 0.97.

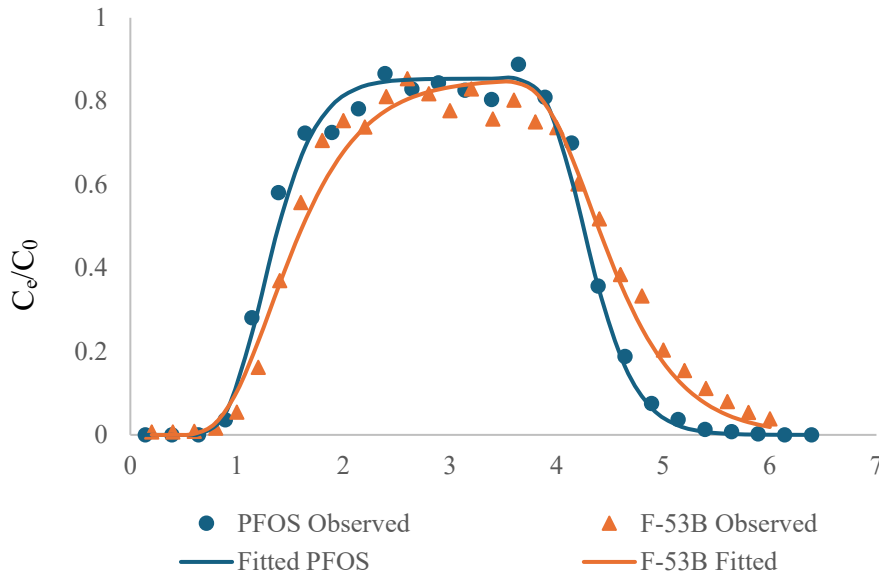


Figure 3. Individual transport BTCs and model fitting for PFOS and 6:2 Cl-PFESA

Following individual transport experiments, the PFOS and 6:2 Cl-PFESA co-transport experiment was conducted. Corresponding BTCs are presented in Figure 4. Distinct fate-and-

transport behaviors were observed in the co-transport between PFOS and 6:2 Cl-PFESA. For PFOS, the co-transport BTC is similar to that of the individual transport, with similar BTC shapes (Figure 4). However, PFOS recovery in the co-transport scenario increased from 86% to 89%, and the BTC plateaus elevated from around 0.85 to around 0.90. These observations suggested less PFOS retardation with the presence of 6:2 Cl-PFESA. Moreover, the PFOS BTC tail is less obvious in the co-transport scenario indicating a lower level of kinetic adsorption process during the co-transport. As compared to PFOS, 6:2 Cl-PFESA achieved an even higher mobility in the co-transport scenario. The recovery significantly increased from 81% to 95% (Table 3). The 6:2 Cl-PFESA BTC was also remarkably changed to a symmetric shape in co-transport (Figure 4) without the long-tailing effect observed in the individual transport.

In terms of the simulation, PFOS BTC in individual and co-transport have comparable parameters estimation. The minor changes are likely caused by the small increase in recovery. As to 6:2 Cl-PFESA, the co-transport BTC has a partitioning coefficient close to 1 and a negligible mass transfer rate, which leads to the decrease in the retardation factor from 2.1 to 1.5. The simulation for PFOS and 6:2 Cl-PFESA in the co-transport scenario achieved excellent fitting, with an R^2 of 0.978 and 0.985, respectively (Table 3).

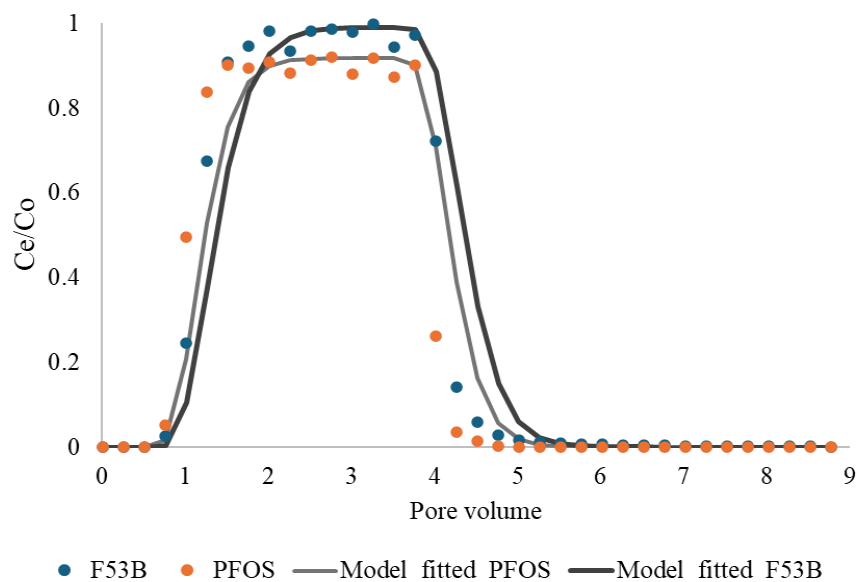


Figure 4. Co-transport BTCs and model fitting for PFOS and 6:2 Cl-PFESA

Table 3. PFAS transport simulation results

PFAS	Recovery	β	ω	μ_1	Retardation factor	R^2
6:2 Cl-PFESA	81%	0.843	7.9E-2	1.3E-2	2.1	0.982
PFOS	86%	0.909	6.4E-2	1.4E-2	1.6	0.992
6:2 Cl-PFESA mix	95%	0.979	1.0E-6	9.4E-3	1.5	0.985
PFOS mix	89%	0.918	2.5E-5	8.5E-2	1.4	0.978

Note: β is the partition coefficient, ω is a dimensionless mass transfer coefficient; μ_1 is the dimensionless deposition coefficient.

3.3 Acute Toxicity

A 96-hour acute toxicity test was conducted to evaluate the impact of PFOA, GenX, and their combined exposure on the mortality rate of zebrafish embryos. The results showed that PFOA had minimal impact on the mortality rate of the embryos when individually exposed at lower concentrations (0.1 $\mu\text{g/L}$ and 1 $\mu\text{g/L}$), with no death observed over the 96-hour exposure period. As the exposure concentration increased, we started to observe embryo death. Specifically, the mortality rate in the PFOA exposure group reached 12.5% at 20 $\mu\text{g/L}$, and 4.2% at both 100 $\mu\text{g/L}$ and 200 $\mu\text{g/L}$ (Figure 5). Unlike the PFOA individual exposure where the highest mortality rate was observed at the medium concentration range, GenX individual exposure led to the highest mortality rate at the highest exposure concentration of 200 $\mu\text{g/L}$. Specifically, the GenX exposure mortality rate increased from 4.2% at 0.1 $\mu\text{g/L}$ and 1 $\mu\text{g/L}$ to 8.33% at 200 $\mu\text{g/L}$ (Figure 5). In the combined exposure group, the mortality rate was only observed from the low to middle concentration range (i.e., 0.1 $\mu\text{g/L}$ to 20 $\mu\text{g/L}$), indicating a potential distinct synergistic toxic effect from the combination of PFOA and GenX (Figure 5c). However, as the concentration further increased to above 20 $\mu\text{g/L}$, the mortality rate was no longer observed. This trend is similar to the mortality rate decrease from the middle to high concentration range in PFOA individual exposure scenarios, which might suggest the dominant effects from PFOA rather than GenX in their combined exposure at a high concentration range.

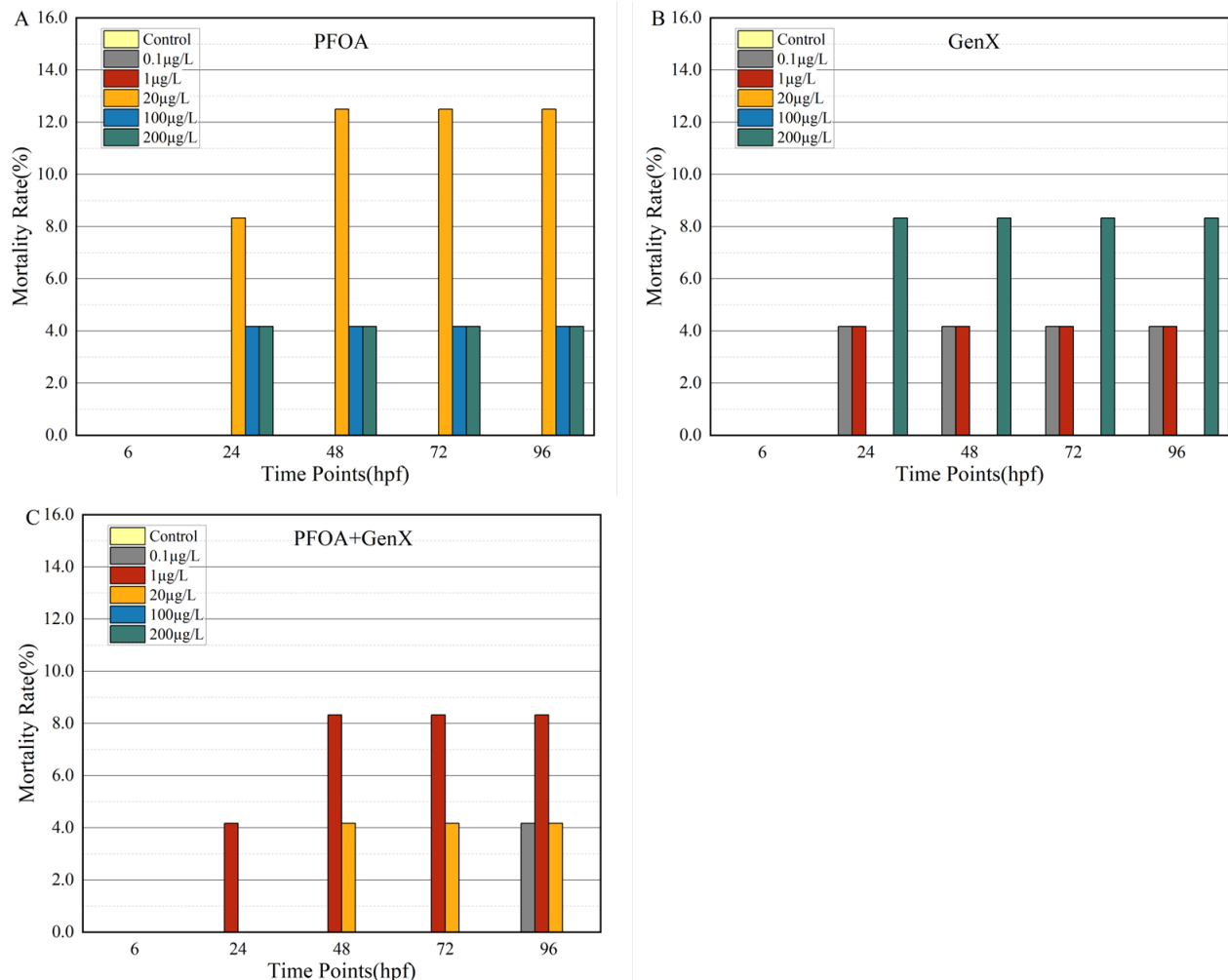


Figure 5. Mortality rate of zebrafish embryos exposed to (a) PFOA, (b) GenX, and (c) the combination of PFOA and GenX

The observations suggest that the accumulation of PFAS in the environment could pose lethal threats to aquatic life. Notably, under combined exposure conditions, the mortality rate significantly increased even at lower concentrations (i.e., 0.1 µg/L and 1 µg/L), suggesting a potential synergistic toxic effect between PFOA and GenX. This synergistic effect implies that even at relatively low concentrations, the presence of these compounds together can lead to severe toxic reactions, raising concerns for environmental risk assessment (Wang et al. 2023). It needs to be noted that the current project contains a relatively small sample size at each level of exposure (n=24). Such a limitation may suppress the trend of exposure impacts under certain PFAS levels, and therefore future studies with larger sample sizes may need to confirm the observations from the current project.

The results for the malformation rate revealed that exposure to PFOA and GenX induced developmental abnormalities in the embryos, particularly at higher concentrations. In the PFOA exposure group, the malformation rate significantly increased at the highest concentration of 200 $\mu\text{g/L}$, reaching a maximum rate of 12.5%. In the GenX exposure group, the malformation rate was 8.33% at concentrations of 20 $\mu\text{g/L}$ and 200 $\mu\text{g/L}$ (Figure 6). Unlike the observation for the mortality rate, the malformation of zebrafish embryos under PFAS exposure is both concentration and time dependent. At 24 hpf, only PFOA exposure at 200 $\mu\text{g/L}$ caused malformation. As exposure time increased, more malformation developed for zebrafish embryos at lower concentration for both PFOA and GenX individual exposure (Figure 6c). In the combined exposure group, the malformation rate increased significantly at concentrations of 1 $\mu\text{g/L}$ and above, particularly at 100 $\mu\text{g/L}$, where the highest malformation rate was 8.3%. It is interesting that a lower malformation rate was observed in combined exposure scenarios. But it should be noted that the combined exposure led to malformation at an early development stage (i.e., 24 hpf) at a low concentration range, which might suggest an increased risk of malformation occurrence. The types of malformations observed included spinal curvature, cardiac edema, and other developmental abnormalities, which could negatively affect the long-term health and reproductive capabilities of the organisms, suggesting that PFASs may have profound impacts on aquatic ecosystems (Lu et al. 2014).

The experimental observation also revealed developmental delays in zebrafish embryos exposed to PFOA, GenX, and their combination (Figure 7). The embryos failed to reach the expected developmental stages within 96 hours in middle to high exposure concentrations (i.e., 20 to 200 $\mu\text{g/L}$) (Table 4). The developmental delays were similar in the two individual exposure groups. In the co-exposure group, more notable developmental delay was observed in the middle exposure range (i.e., 20 to 100 $\mu\text{g/L}$). Potential synergistic effects from PFOA and GenX co-exposure might lead to the observed worse developmental delay in the middle concentration range.

This finding suggests that PFOA and GenX may disrupt critical developmental processes such as cell division, tissue differentiation, and organ formation, leading to developmental delays in organisms (Wallace et al. 2005). Developmental delays not only affect survival and health during the embryonic stage but could also have long-term consequences on individual growth and reproductive capacity, and therefore should be considered a crucial endpoint in environmental toxicity assessments to evaluate comprehensively the potential hazards of PFAS exposure.

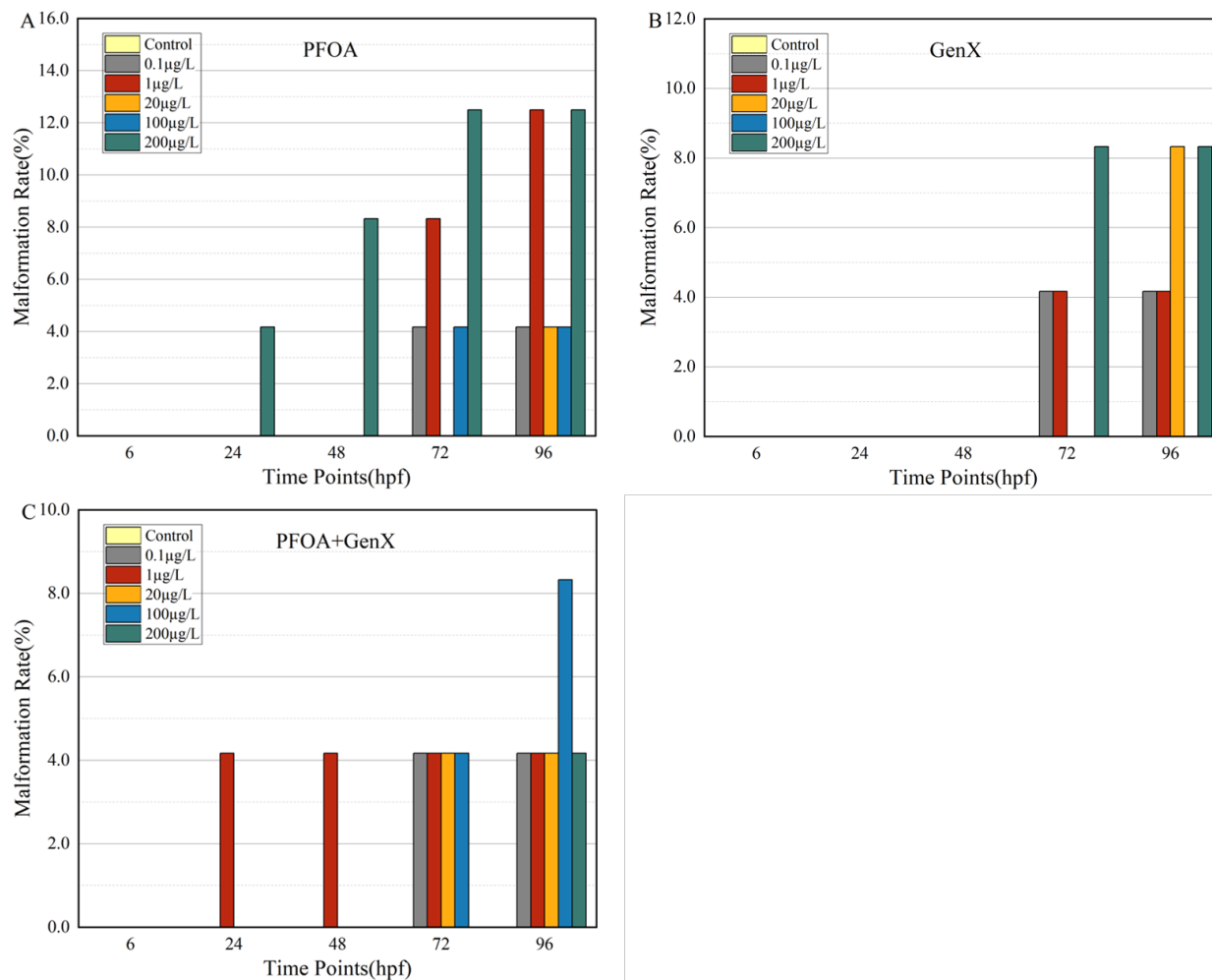


Figure 6. Malformation rate of zebrafish embryos exposed to (a) PFOA, (b) GenX, and (c) the combination of PFOA and GenX

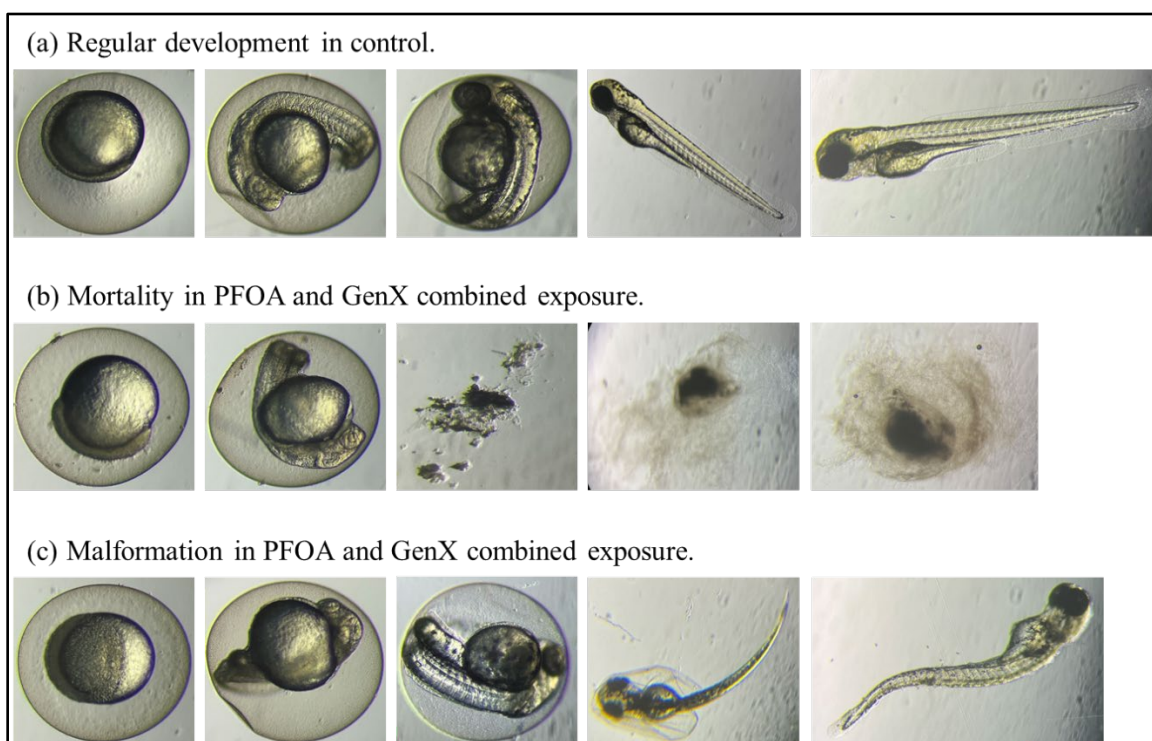


Figure 7. Zebrafish embryo development under combined exposure of PFOA and GenX

Table 4. Apical observations of developmental delays in zebrafish embryos acutely exposed to PFOA, GenX, and their combination within 96 hours post-fertilization

Concentration (µg/L)	Control	0.1	1	20	100	200
PFOA				+	+	+
GenX				+	+	+
PFOA + GenX				+++++	++	+

3.4 Chronic Toxicity

This test evaluated the effects of co-exposure to different concentrations of PFOA and GenX on the expression of key liver genes (*cyp1a*, *il6*, *vtg1*, and *fabp10a*) in female zebrafish. The expression levels of the four liver genes are presented in Figure 8. The results demonstrate that co-exposure to PFOA and GenX leads to a significant upregulation of *cyp1a*, *il6*, *vtg1*, and *fabp10a* gene expression in the liver of female zebrafish, with the magnitude of these changes being dose dependent.

The expression levels of both *cyp1a* and *il6* increased significantly with higher concentrations of PFOA and GenX. In the control group, the expression levels of *cyp1a* and *il6* were 1.031 and 1.050, respectively. In the 0.2 µg/L, 20 µg/L, and 200 µg/L exposure groups, *cyp1a* expression levels were elevated to 1.402, 2.654, and 7.354, while *il6* expression levels increased to 2.819, 3.971, and 5.053, respectively. Compared to the control group, these changes were statistically significant in the 20 µg/L and 200 µg/L exposure groups ($p < 0.05$) (Figure 8a). These findings suggest that higher concentrations of PFOA and GenX co-exposure strongly induce liver detoxification processes and inflammatory responses in zebrafish.

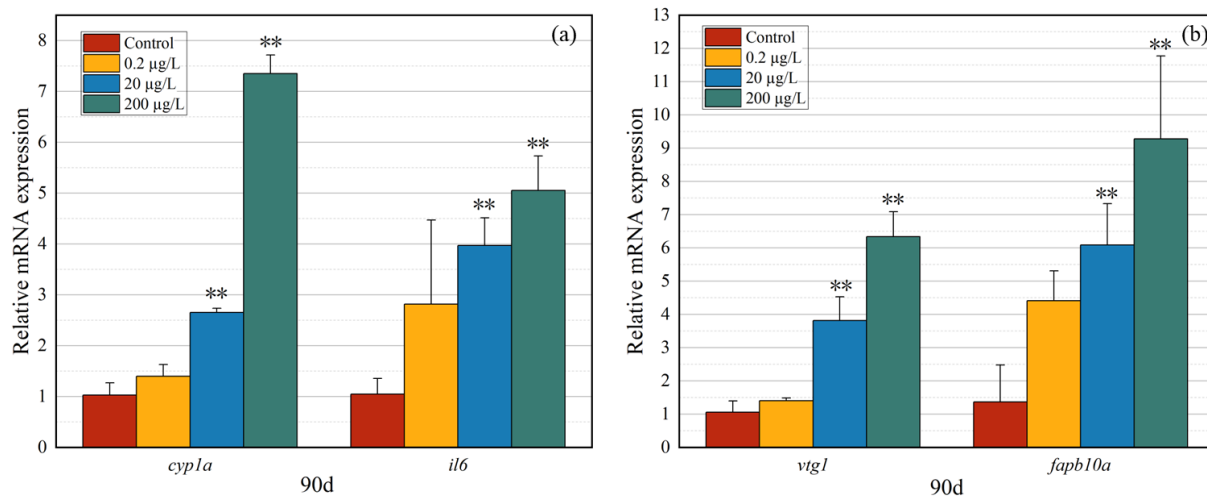


Figure 8. Effects of combined exposure to PFOA and GenX at different concentrations on the expression of liver genes (a) *cyp1a* and *il6* gene, and (b) *vtg1* and *fabp10a* gene

The expression of *vtg1* and *fabp10a* also showed significant upregulation with increasing concentrations of PFOA and GenX. In the control group, the expression levels of *vtg1* and *fabp10a* were 1.063 and 1.369, respectively. In the 0.2 µg/L, 20 µg/L, and 200 µg/L exposure groups, *vtg1* expression levels increased to 1.408, 3.815, and 6.339, while *fabp10a* expression levels were raised to 4.415, 6.092, and 9.284, respectively. The differences in gene expression between the control group and the 20 µg/L and 200 µg/L exposure groups were statistically significant ($p < 0.05$) (Figure 8b). The upregulation of these genes suggests that co-exposure to PFOA and GenX may adversely affect the reproductive system and induce strong stress responses in the liver, particularly at higher concentrations.

Significant upregulation of *cyp1a*, *il6*, *vtg1*, and *fabp10a* genes was observed, especially at higher concentrations, indicating dose-dependent toxicity. The gene, *cyp1a*, closely associated with

detoxification, was markedly increased, suggesting an attempt by the liver to counteract the toxicity of these perfluorinated compounds through enhanced expression of detoxification enzymes (Terelius et al. 1993). However, this could lead to an overburdened metabolic system and further cellular damage. The *il6* gene, a marker for inflammation, also showed increased expression particularly at the highest concentration, highlighting a potential inflammatory response which could lead to tissue damage or liver disease (Del Campo et al. 2018). The upregulation of *vtg1* indicates potential endocrine disruption affecting reproductive functions, which could adversely affect population sustainability and ecological balance (Hou et al. 2016). Similarly, the increase in *fabp10a* expression suggests a significant stress response, potentially leading to apoptosis or other cellular damage, particularly under high exposure conditions (Venkatachalam et al. 2012). Collectively, the findings indicate a synergistic toxic effect when exposure to both compounds occurs together, with possible pathways including increased detoxification load, inflammatory response, and endocrine disruption, ultimately leading to severe liver damage. While this study highlights some significant effects of combined PFOA and GenX exposure, limitations include its focus solely on gene expression changes without assessing how these translate to protein levels and specific physiological impacts. Future research should consider responses in male zebrafish and assess long-term population dynamics and ecosystem impacts.

3.5 Discussion

In general, the key findings from this study have significant implications for future PFAS risk assessment and management efforts. The observed enhancement of PFAS alternative's transport in the co-transport scenario suggests that regulatory frameworks should consider the interactive effects of different PFAS compounds rather than evaluating them in isolation. This is particularly important when assessing the exposure risks of PFAS alternatives, as their mobility and persistence in the environment could be underestimated if studied independently. Additionally, toxicity results from zebrafish exposure experiments underscore the necessity of incorporating synergistic effects into health risk assessments. The PFAS compound-dependent liver impacts further emphasize the need for refining toxicity thresholds based on co-exposure scenarios.

For water-scarce regions like New Mexico, people rely on groundwater as their primary drinking water source. Given that the research demonstrated the enhanced transport of certain novel

PFAS due to co-occurrence effects, water managers in New Mexico should anticipate the potential for widespread contamination in aquifers, particularly in areas where PFAS sources are present. Moreover, the observed toxicity of PFAS mixtures highlights the urgency of ensuring that drinking water treatment methods effectively remove multiple PFAS simultaneously. Future research should also explore how PFAS behave under the unique geochemical conditions for alternative water resources in water-scarce regions, such as brackish groundwater and produced water.

Despite these valuable findings, this study has certain limitations that need to be addressed in future research. First of all, a relatively high PFAS concentration (i.e., 200 µg/L) was used in the transport experiment, which exceeds the PFAS levels typically detected in most real-world environmental samples. While this approach allowed for a clear observation of transport behaviors, it may limit the direct applicability of the results to management and risk assessments under lower PFAS exposure scenarios. Additionally, the exposure experiments involved a relatively small sample size (i.e., n=24), which restricts the statistical robustness of the observed toxicity patterns. Larger-scale studies are necessary to confirm the observed effects and improve the reliability of dose-response relationships for risk characterization.

Future research should address these limitations and further explore key areas of PFAS transport and toxicity. Advancing metabolomics and proteomics approaches could provide deeper insights into PFAS-induced biochemical disruptions in exposed organisms, particularly in aquatic ecosystems where PFAS contamination is prevalent. Additionally, investigating microbiome-mediated effects in both natural systems and organic tissues could reveal potential microbial interactions that influence PFAS pathway and toxicity. From a remediation perspective, developing selective adsorbents with enhanced specificity for various PFAS structures remains a priority to improve removal efficiency. Lastly, expanding toxicity studies to include larger sample sizes and transport studies to a broader range of geochemical conditions would help verify the findings from the current project. Such future efforts would contribute to a more comprehensive understanding of PFAS risks and inform more effective management strategies.

4 CONCLUSIONS

This study conducted a review to summarize the occurrence of conventional PFAS and their novel alternatives in groundwater and surface water, completed column experiments to investigate the collective effects of PFAS co-occurrence on their fate-and-transport behaviors, and conducted toxicity experiments to estimate the collective effects of PFAS co-exposure on zebrafish development. The review identified over 100 PFAS occurrence records and compared their occurrence in groundwater and surface water. According to the review, conventional PFAS have a more widespread occurrence, and a higher level of occurrence compared to novel alternatives, which contribute to ongoing PFAS challenges. We did not identify as much literature data regarding novel PFAS especially in groundwater; however, it is also present although likely at lower levels than traditional PFAS in Asian surface waters.

For the transport experiments, PFAS individual and co-transport BTCs were obtained from the experiments and fitted with an advection dispersion transport model. The BTC observation and fate-and-transport parameters estimation process indicated the impacts of PFAS co-occurrence on the mobility of 6:2 Cl-PFESA in the sediment column. Specifically, 6:2 Cl-PFESA had more obvious retardation as compared to PFOS in the individual transport scenarios, while the mobility of 6:2 Cl-PFESA was significantly increased in the co-transport, which could be caused by the competition among PFAS for the limited kinetic adsorption sites.

Regarding the toxicity tests, the acute toxicity test revealed that PFOA and GenX significantly increased mortality and malformation rates at higher concentrations, with a dose-dependent relationship. Synergistic toxic effects were observed under combined exposure, leading to higher mortality, malformation rates, and developmental delay even at lower concentration levels. (We also anticipate that individual PFOA or GenX would also upregulate gene expression even though this study did not involve such tests.) These findings highlight the potential health risks posed by PFAS.

5 REFERENCES

- Ahrens, L., 2011. Polyfluoroalkyl compounds in the aquatic environment: A review of their occurrence and fate. *Journal of Environmental Monitoring*, 13:1:20-31.
- Bai, X. and Son, Y., 2021. Perfluoroalkyl substances (PFAS) in surface water and sediments from two urban watersheds in Nevada, USA. *Science of the Total Environment*, 751:141622.
- Brendel, S., Fetter, É., Staude, C., Vierke, L., and Biegel-Engler, A., 2018. Short-chain perfluoroalkyl acids: Environmental concerns and a regulatory strategy under REACH. *Environmental Sciences Europe*, 30:1:1-11.
- Brusseau, M.L., Anderson, R.H., and Guo, B., 2020. PFAS concentrations in soils: Background levels versus contaminated sites. *Science of the Total Environment*, 740:140017.
- Del Campo, J.A., Gallego, P., and Grande, L., 2018. Role of inflammatory response in liver diseases: Therapeutic strategies. *World Journal of Hepatology*, 10:1:1.
- DeWitt, J.C., Peden-Adams, M.M., Keller, J.M., and Germolec, D.R., 2012. Immunotoxicity of perfluorinated compounds: Recent developments. *Toxicologic Pathology*, 40:2:300-311.
- Dorts, J., Kestemont, P., Marchand, P.A., D'Hollander, W., Thézenas, M.L., Raes, M., and Silvestre, F., 2011. Ecotoxicoproteomics in gills of the sentinel fish species, *Cottus gobio*, exposed to perfluorooctane sulfonate (PFOS). *Aquatic Toxicology*, 103:1-2:1-8.
- Goosey, E. and Harrad, S., 2012. Perfluoroalkyl substances in UK indoor and outdoor air: Spatial and seasonal variation, and implications for human exposure. *Environment International*, 45:86-90.
- Guo, B., Zebda, R., Drake, S.J., and Sayes, C.M., 2009. Synergistic effect of co-exposure to carbon black and Fe₂O₃ nanoparticles on oxidative stress in cultured lung epithelial cells. *Particle and Fibre Toxicology*, 6:1:1-13.
- Hou, J., Li, L., Wu, N., Su, Y., Lin, W., Li, G., and Gu, Z., 2016. Reproduction impairment and endocrine disruption in female zebrafish after long-term exposure to MC-LR: A life cycle assessment. *Environmental Pollution*, 208:477-485.
- Huang, L., Jin, Q., Tandon, P., Li, A., Shan, A., and Du, J., 2018. High-resolution insight into the competitive adsorption of heavy metals on natural sediment by site energy distribution. *Chemosphere*, 197:411-419.
- Kirchgeorg, T., Dreyer, A., Gabrielli, P., Gabrieli, J., Thompson, L.G., Barbante, C., and Ebinghaus, R., 2016. Seasonal accumulation of persistent organic pollutants on a high altitude glacier in the Eastern Alps. *Environmental Pollution*, 218:804-812.
- Lee, J.W., Lee, J-W., Kim, K., Shin, Y.J., Kim, J., Kim, S., Kim, H., Kim, P., and Park, K., 2017. PFOA-induced metabolism disturbance and multi-generational reproductive toxicity in *Oryzias latipes*. *Journal of Hazardous Materials*, 340:231-240.
- Li, R., Ibeanusi, V., Hoyle-Gardner, J., Crandall, C., Jagoe, C., Seaman, J., Anandhi, A., and Chen, G., 2019a. Bacterial-facilitated uranium transport in the presence of phytate at Savannah River Site. *Chemosphere*, 223:351-357.
- Li, R., Wei, C., Cheng, H., and Chen, G., 2019b. Adhesion of Colloids and Bacteria to Porous Media: A Critical Review. *Reviews of Adhesion and Adhesives*, 7:4:417-459.

- Li, R., Zhang, Z., Li, S., Tang, Y., Wei, C. and Chen, G., 2019c. Cadmium–bacteria complexation and subsequent bacteria-facilitated cadmium transport in saturated porous media. *Journal of Environmental Quality*, 48:5:1524-1533.
- Lu, Z.-G., Li, M.-H., Wang, J.-S., Wei, D.-D., Liu, Q.-W., and Kong, L.-Y., 2014. Developmental toxicity and neurotoxicity of two matrine-type alkaloids, matrine and sophocarpine, in zebrafish (*Danio rerio*) embryos/larvae. *Reproductive Toxicology*, 47:33-41.
- Munoz, G., Labadie, P., Botta, F., Lestremieu, F., Lopez, B., Geneste, E., Pardon, P., Dévier, M.H., and Budzinski, H., 2017. Occurrence survey and spatial distribution of perfluoroalkyl and polyfluoroalkyl surfactants in groundwater, surface water, and sediments from tropical environments. *Science of the Total Environment*, 607:243-252.
- OECD, T.N., 2013. 236: Fish embryo acute toxicity (FET) test. *OECD Guidelines for the Testing of Chemicals*, Section, 2, pp.1-22.
- Pelch, K.E., Reade, A., Wolffe, T.A., and Kwiatkowski, C.F., 2019. PFAS health effects database: Protocol for a systematic evidence map. *Environment International*, 130, p. 104851.
- Podder, A., Sadmani, A.A., Reinhart, D., Chang, N.B., and Goel, R., 2021. Per and poly-fluoroalkyl substances (PFAS) as a contaminant of emerging concern in surface water: A transboundary review of their occurrences and toxicity effects. *Journal of Hazardous Materials*, 419:126361.
- Qi, L., Li, R., Wu, Y., Lin, X., and Chen, G., 2022. Effect of solution chemistry on the transport of short-chain and long-chain perfluoroalkyl carboxylic acids (PFCAs) in saturated porous media. *Chemosphere*, 303:135160.
- Steenland, K. and Winquist, A., 2021. PFAS and cancer, a scoping review of the epidemiologic evidence. *Environmental Research*, 194:110690.
- Terelius, Y., Lindros, K., Albano, E., and Ingelman-Sundberg, M., 1993. Isozyme-specificity of cytochrome P450-mediated hepatotoxicity. *Frontiers Biotransformation*, 8:186-231.
- Toride, N., Leij, F.J., and Van Genuchten, M.T., 1995. The CXTFIT code for estimating transport parameters from laboratory or field tracer experiments (Vol. 2). Riverside, CA: US Salinity Laboratory.
- U.S. EPA, 2021. Draft Method 1633: Analysis of Per- and Polyfluoroalkyl Substances (PFAS) in Aqueous, Solid, Biosolids, and Tissue Samples by LC-MS/MS. <https://www.epa.gov/system/files/documents/2024-12/method-1633a-december-5-2024-508-compliant.pdf>. Accessed on February 27, 2025.
- U.S. EPA, 2024. Final PFAS National Primary Drinking Water Regulation. <https://www.epa.gov/sdwa/and-polyfluoroalkyl-substances-pfas>. Accessed on February 27, 2025.
- van Genuchten, M.T., 1981. Analytical solutions for chemical transport with simultaneous adsorption, zero-order production and first-order decay. *Journal of Hydrology*, 49:3-4:213-233.
- Venkatachalam, A.B., Lall, S.P., Denovan-Wright, E.M., and Wright, J.M., 2012. Tissue-specific differential induction of duplicated fatty acid-binding protein genes by the peroxisome proliferator, clofibrate, in zebrafish (*Danio rerio*). *BMC Evolutionary Biology*, 12:1-14.

- Wallace, K.N., Akhter, S., Smith, E.M., Lorent, K., and Pack, M., 2005. Intestinal growth and differentiation in zebrafish. *Mechanisms of Development*, 122:2:157-173.
- Wang, X., Zhang, W., Lamichhane, S., Dou, F., and Ma, X., 2023. Effects of physicochemical properties and co-existing zinc agrochemicals on the uptake and phytotoxicity of PFOA and GenX in lettuce. *Environmental Science and Pollution Research*, 30:15:43833-43842.
- Xin, X., Chen, B., Yang, M., Gao, S., Wang, H., Gu, W., Li, X., and Zhang, B., 2023. A critical review on the interaction of polymer particles and co-existing contaminants: Adsorption mechanism, exposure factors, effects on plankton species. *Journal of Hazardous Materials*, 445, p.130463.

6 APPENDICES

Appendix 1: PFOA Occurrence

Study	Location	Matrix	Species	Concentration, ng/L			Number of Measurements	Year	Contamination
				Min	Max	Average			
Monthly Variations in Perfluorinated Compound Concentrations in Groundwater	Alaska, US	Groundwater	PFOA	0.07	0.13	0.1	54	2016-2017	-
Contamination of groundwater with per- and polyfluoroalkyl substances (PFAS) from legacy landfills in an urban re-development precinct	Melbourne, Australia	Groundwater	PFOA	2	74	12	13	2019	Landfills
Distribution, source identification and health risk assessment of PFASs in groundwater from Jiangxi Province, China	southeastern China	Groundwater	PFOA	-	74	2.5	88	2016	-
Occurrence and Risk Assessment of Perfluorooctanoate (PFOA) and Perfluorooctane Sulfonate (PFOS) in Surface Water, Groundwater and Sediments of the Jin River Basin, Southeastern China	Jin River Basin, China	Groundwater	PFOA	0.26	151	3.41	16	2020	-
Occurrence and Distribution of Per- and Polyfluoroalkyl Substances in Tianjin, China: The Contribution of Emerging and Unknown Analogues	Haihe River, and Duliujian River, Tianjin, China	Groundwater	PFOA	-	48	-	49	2018	-
Contamination of per- and polyfluoroalkyl substances in the water source from a typical agricultural area in North China	Beijing and Tianjin, North China	Groundwater	PFOA	-	7.585	7.585	16	2014	-
Per- and polyfluoroalkyl substances (PFASs) in groundwater by ultrahigh performance liquid chromatography coupled with quadrupole orbitrap high resolution mass spectrometry	Hebei Province, China	Groundwater	PFOA	-	19.3	1.4	30	2017	-
Occurrence survey and spatial distribution of perfluoroalkyl and polyfluoroalkyl surfactants in groundwater, surface water, and sediments from tropical environments	Guadeloupe, Leeward Islands	Groundwater	PFOA	-	15	0.71	75	2012	-

Occurrence survey and spatial distribution of perfluoroalkyl and polyfluoroalkyl surfactants in groundwater, surface water, and sediments from tropical environments	Martinique, Leeward Island	Groundwater	PFOA	-	14	1.1	80	2012	-
Distribution, source identification and health risk assessment of PFASs and two PFOS alternatives in groundwater from non-industrial areas	Jiangsu province, China	Groundwater	PFOA	-	49.3	5.59	102	2016	Domestic sewage
Occurrence and Risk Assessment of Perfluorooctanoate (PFOA) and Perfluorooctane Sulfonate (PFOS) in Surface Water, Groundwater and Sediments of the Jin River Basin, Southeastern China	Jin River Basin, China	Surface water	PFOA	0.26	15.1	5.67	16	2020	-
Seasonal Changes of PFOS and PFOA Concentrations in Lake Biwa Water	Northern Lake Biwa, Japan	Surface water	PFOA	7	10	-	8	2009	-
Seasonal Changes of PFOS and PFOA Concentrations in Lake Biwa Water	Southern Lake Biwa, Japan	Surface water	PFOA	8.3	13	-	4	2009	-
Seasonal Changes of PFOS and PFOA Concentrations in Lake Biwa Water	Akanoi Bay, Japan	Surface water	PFOA	9.1	17	-	8	2009	-
Seasonal Changes of PFOS and PFOA Concentrations in Lake Biwa Water	Akanoi Bay, Japan	Surface water	PFOA	12	26	-	168	2009	-
PFOS and PFOA in environmental and tap water in China	China	Surface water	PFOA	-	1.3	0.1	13	-	-
Temporal trend of perfluorinated compounds in untreated wastewater and surface water in the middle part of the Danube River belonging to the northern part of Serbia	Serbia	Surface water	PFOA	8.85	14.2	12.1	12	-	Wastewater treatment plant
Analysis of 58 poly-/perfluoroalkyl substances and their occurrence in surface water in a high-technology industrial park	Shanghai, China	Surface water	PFOA	12.9	55.7	32.9	-	-	Industrial park
Occurrence and distribution of perfluoroalkyl acids (PFAAs) in surface water and sediment of a tropical coastal area (Bay of Bengal coast, Bangladesh)	Bangladesh	Surface water	PFOA	3.18	27.83	12.4	14	2015	-

Occurrence and distribution of perfluoroalkyl acids (PFAAs) in surface water and sediment of a tropical coastal area (Bay of Bengal coast, Bangladesh)	Bangladesh	Surface water	PFOA	3.17	24.8	11.6	14	2015	-
Perfluorinated compounds in surface waters from Northern China: Comparison to level of industrialization	Liaoning, China	Surface water	PFOA	2.6	82	27	10	2012	-
Perfluorinated compounds in surface waters from Northern China: Comparison to level of industrialization	Tianjin, China	Surface water	PFOA	3	12	6.8	8	2007	-
Perfluorinated compounds in surface waters from Northern China: Comparison to level of industrialization	Shanxi, China	Surface water	PFOA	0.43	15	2.7	9	2012	-
Perfluorinated compounds in surface waters from Northern China: Comparison to level of industrialization	Hohhot, China	Surface water	PFOA	0.8	1.8	1.2	8	2006	-
Perfluorinated compounds in surface waters from Northern China: Comparison to level of industrialization	Guanting, China	Surface water	PFOA	0.55	2.3	1.2	7	2012	-
Survey of per- and polyfluoroalkyl substances (PFAS) in surface water collected in Pensacola, FL	Pensacola, Florida, US	Surface water	PFOA	0.3	19	0.97	45	2020	-
Increased levels of perfluorooctanesulfonic acid (PFOS) during Hurricane Dorian on the east coast of Florida	Matanzas River, Florida, US	Surface water	PFOA	0.38	0.5	0.4	10	2019-2021	-
Per- and polyfluoroalkyl substances in source and treated drinking waters of the United States	US	Surface water	PFOA	-	112	6.32	24	2017	-
Contamination of perfluorooctane sulfonate (PFOS) and perfluorooctanoate (PFOA) in surface water of the Yodo River basin (Japan)	Yodo R. basin, Japan	Surface water	PFOA	0.6	49	2.4	18	2004	Sewage treatment plant
Contamination of perfluorooctane sulfonate (PFOS) and perfluorooctanoate (PFOA) in surface water of the Yodo River basin (Japan)	Yodo R. basin, Japan	Surface water	PFOA	0.4	56	3.8	30	2005	Sewage treatment plant

Contamination of perfluorooctane sulfonate (PFOS) and perfluorooctanoate (PFOA) in surface water of the Yodo River basin (Japan)	Yodo R. basin, Japan	Surface water	PFOA	0.8	123	5.6	33	2005	Sewage treatment plant
Determination of perfluorinated compounds (PFCs) in solid and liquid phase river water samples in Chao Phraya River, Thailand	Chao Phraya River, Thailand	Surface water	PFOA	-	-	10.7	6	2008	-
Determination of perfluorinated compounds (PFCs) in solid and liquid phase river water samples in Chao Phraya River, Thailand	Chao Phraya River, Thailand	Surface water	PFOA	-	-	1.4	6	2008	-
Perfluorooctane Sulfonate Concentrations in Surface Water in Japan	Japan	Surface water	PFOA	0.2	0.3	0.25	7	2002	-
Discovery of a Novel Polyfluoroalkyl Benzenesulfonic Acid around Oilfields in Northern China	Heilongjiang, China	Surface Water	PFOA	2.7	28	12	77	2015	Oil fields
Discovery of a Novel Polyfluoroalkyl Benzenesulfonic Acid around Oilfields in Northern China	Heilongjiang, China	Surface Water	PFOA	4	13	6.8	94	2015	Oil fields
Emissions, Isomer-Specific Environmental Behavior, and Transformation of OBS from One Major Fluorochemical Manufacturing Facility in China	Jiangsu, China	Surface Water	PFOA	7.04	82.2	17.4	24	2017	Fluorochemical facility
Occurrence and Distribution of Per- and Polyfluoroalkyl Substances in Tianjin, China: The Contribution of Emerging and Unknown Analogues	Tianjin, China	Surface Water	PFOA	0.88	200	-	49	2018	-
Spatiotemporal distribution, partitioning behavior and flux of per- and polyfluoroalkyl substances in surface water and sediment from Poyang Lake, China	Boyang Lake, Jiangxi, China	Surface Water	PFOA	1.8	17	-	10	2019	Fluorochemical facility, fire station, and metal plating site

Appendix 2: PFOS Occurrence

Study	Location	Matrix	Species	Concentration, ng/L			Number of Measurements	Year	Contamination
				Min	Max	Average			
Monthly Variations in Perfluorinated Compound Concentrations in Groundwater	Alaska, US	Groundwater	PFOS	0.03	0.055	0.04	54	2016-2017	-
Occurrence and Risk Assessment of Perfluorooctanoate (PFOA) and Perfluorooctane Sulfonate (PFOS) in Surface Water, Groundwater and Sediments of the Jin River Basin, Southeastern China	Jin River Basin, China	Groundwater	PFOS	-	7.01	0.58	16	2020	-
Distribution, source identification and health risk assessment of PFASs in groundwater from Jiangxi Province, China	Jiangxi, China	Groundwater	PFOS	-	33.8	1.6	88	2016	-
Perfluorooctane Sulfonic Acid (PFOS) in River Water and Groundwater along Bharathapuzha River Basin, India	Kerala, India	Groundwater	PFOS	0	1	0.2	26	2021	-
Occurrence and Distribution of Per- and Polyfluoroalkyl Substances in Tianjin, China: The Contribution of Emerging and Unknown Analogues	Tianjin, China	Groundwater	PFOS	-	2.9	-	49	2018	-
Contamination profiles and risk assessment of per- and polyfluoroalkyl substances in groundwater in China	Hebei, China	Groundwater	PFOS	-	-	0.1	44	2014-2015	-
A sensitive method for simultaneous determination of 12 classes of per- and polyfluoroalkyl substances (PFASs) in groundwater by ultrahigh performance liquid chromatography coupled with	Hebei, China	Groundwater	PFOS	-	0.775	0.2	30	2017	-
Distribution, source identification and health risk assessment of PFASs and two PFOS alternatives in groundwater from non-industrial areas	Jiangsu, China,	Groundwater	PFOS	0.26	79	5.1	12	2016	Sewage
Contamination profiles and risk assessment of per- and polyfluoroalkyl substances in groundwater in China	China	Groundwater	PFOS	-	-	0.2	56	2014-2016	-

Contamination profiles and risk assessment of per- and polyfluoroalkyl substances in groundwater in China	Gansu, China	Groundwater	PFOS	-	-	0.65	30	2014-2017	-
Contamination profiles and risk assessment of per- and polyfluoroalkyl substances in groundwater in China	Qinghai, China	Groundwater	PFOS	-	-	0.75	39	2014-2018	-
Preferential Retention and Transport of Perfluorooctanesulfonic Acid in a Dolomite Aquifer	Pennsylvania, US	Groundwater	PFOS	0.42	300	-	8	2016-2018	-
Occurrence and Risk Assessment of Perfluorooctanoate (PFOA) and Perfluorooctane Sulfonate (PFOS) in Surface Water, Groundwater and Sediments of the Jin River Basin, Southeastern China	Jin River Basin, China	Surface water	PFOS	-	2.56	-	16	2020	-
Seasonal Changes of PFOS and PFOA Concentrations in Lake Biwa Water	Northern Lake Biwa, Japan	Surface water	PFOS	7	10	-	8	2009	-
Seasonal Changes of PFOS and PFOA Concentrations in Lake Biwa Water	Southern Lake Biwa, Japan	Surface water	PFOS	8.3	13	-	4	2009	-
Seasonal Changes of PFOS and PFOA Concentrations in Lake Biwa Water	Akanoi Bay, Japan	Surface water	PFOS	9.1	17	-	8	2009	-
Seasonal Changes of PFOS and PFOA Concentrations in Lake Biwa Water	Akanoi Bay, Japan	Surface water	PFOS	12	26	-	168	2009	-
Temporal trend of perfluorinated compounds in untreated wastewater and surface water in the middle part of the Danube River belonging to the northern part of Serbia	Serbia	Surface water	PFOS	4.36	14.9	6.11	12	-	Wastewater treatment plant
Analysis of 58 poly-/perfluoroalkyl substances and their occurrence in surface water in a high-technology industrial park	Shanghai, China	Surface water	PFOS	1.54	24.9	4.4	-	-	Industrial park
Occurrence and distribution of perfluoroalkyl acids (PFAAs) in surface water and sediment of a tropical coastal area (Bay of Bengal coast, Bangladesh)	Bangladesh	Surface water	PFOS	<LOD	5.1	1.45	14	2015	-
Occurrence and distribution of perfluoroalkyl acids (PFAAs) in surface water and sediment of a tropical coastal area (Bay of Bengal coast, Bangladesh)	Bangladesh	Surface water	PFOS	0.16	4.26	1.02	14	2015	-
Perfluorinated compounds in surface waters from Northern China: Comparison to level of industrialization	Liaoning, China	Surface water	PFOS	-	31	4.7	10	2012	-

Perfluorinated compounds in surface waters from Northern China: Comparison to level of industrialization	Tianjin, China	Surface water	PFOS	0.09	11	2.6	8	2007	-
Perfluorinated compounds in surface waters from Northern China: Comparison to level of industrialization	Shanxi, China	Surface water	PFOS	-	5.7	0.93	9	2012	-
Perfluorinated compounds in surface waters from Northern China: Comparison to level of industrialization	Hohhot, China	Surface water	PFOS	-	1.1	0.32	8	2006	
Perfluorinated compounds in surface waters from Northern China: Comparison to level of industrialization	Qinghai, China	Surface water	PFOS	0.55	2.3	1.2	7	2012	-
Contamination of per- and polyfluoroalkyl substances in the water source from a typical agricultural area in North China	Beijing and Tianjin, China	Surface water	PFOS	-	0.229	0.026	16	2021	-
Environmental and dietary exposure of perfluorooctanoic acid and perfluorooctanesulfonic acid in the Nakdong River, Korea	Nakdong-river, South Korea	Surface water	PFOS	0.047	0.101	0.08	6	2013-2015	-
Increased levels of perfluorooctanesulfonic acid (PFOS) during Hurricane Dorian on the east coast of Florida	Matanzas River, Florida, US	Surface water	PFOS	0.6	1.35	1	9	2019-2020	-
Per- and polyfluoroalkyl substances in source and treated drinking waters of the United States	US	Surface water	PFOS	-	48.3	2.28	24	2017	-
Contamination of perfluorooctane sulfonate (PFOS) and perfluorooctanoate (PFOA) in surface water of the Yodo River basin (Japan)	Yodo R. basin, Japan	Surface water	PFOS	0.6	49	2.4	18	2004	Sewage treatment plant
Contamination of perfluorooctane sulfonate (PFOS) and perfluorooctanoate (PFOA) in surface water of the Yodo River basin (Japan)	Yodo R. basin, Japan	Surface water	PFOS	0.4	56	3.8	30	2005	Sewage treatment plant
Contamination of perfluorooctane sulfonate (PFOS) and perfluorooctanoate (PFOA) in surface water of the Yodo River basin (Japan)	Yodo R. basin, Japan	Surface water	PFOS	0.8	123	5.6	33	2005	Sewage treatment plant
Determination of perfluorinated compounds (PFCs) in solid and liquid phase river water samples in Chao Phraya River, Thailand	Chao Phraya River, Thailand	Surface water	PFOS	-	-	0.8	6	2008	-
Determination of perfluorinated compounds (PFCs) in solid and liquid phase river water samples in Chao Phraya River, Thailand	Chao Phraya River, Thailand	Surface water	PFOS	-	-	0.6	6	2008	-

Perfluorooctane Sulfonate Concentrations in Surface Water in Japan	Japan	Surface water	PFOS	1.32	1.58	1.43	7	2002	-
Discovery of a Novel Polyfluoroalkyl Benzenesulfonic Acid around Oilfields in Northern China	Heilongjiang, China	Surface Water	PFOS	0.07	4.4	0.81	43	2015	Oil fields
Discovery of a Novel Polyfluoroalkyl Benzenesulfonic Acid around Oilfields in Northern China	Heilongjiang, China	Surface Water	PFOS	0.65	150	14	60	2015	Oil fields
Emissions, Isomer-Specific Environmental Behavior, and Transformation of OBS from One Major Fluorochemical Manufacturing Facility in China	Jiangsu, China	Surface Water	PFOS	0.38	2.78	1.58	24	2017	Fluorochemical facility
Occurrence and Distribution of Per- and Polyfluoroalkyl Substances in Tianjin, China: The Contribution of Emerging and Unknown Analogues	Tianjin, China	Surface Water	PFOS	0.42	530	-	49	2018	-
Perfluorooctane Sulfonic Acid (PFOS) in River Water and Groundwater along Bharathapuzha River Basin, India	Kerala, India	Surface water	PFOS	0	1.3	0.4	26	2021	-
Spatiotemporal distribution, partitioning behavior and flux of per- and polyfluoroalkyl substances in surface water and sediment from Poyang Lake, China	Boyang Lake, Jiangxi, China	Surface Water	PFOS	1.4	21	-	10	2019	Fluorochemical facility, fire station, and metal plating site
Tissue distribution and bioaccumulation of a novel polyfluoroalkyl benzenesulfonate in crucian carp	Yubei River, China	Surface Water	PFOS	1.54	2.62	2.04	20	2020	-
Tissue distribution and bioaccumulation of a novel polyfluoroalkyl benzenesulfonate in crucian carp	Gaoneidian Lake, China	Surface Water	PFOS	1.27	1.95	1.61	20	2020	-

Appendix 3: GenX Occurrence

Study	Location	Matrix	Species	Concentration, ng/L			Number of Measurements	Year	Contamination
				Min	Max	Average			
The PFOA substitute GenX detected in the environment near a fluoropolymer manufacturing plant in the Netherlands	Dordrecht, Netherlands	Groundwater	GenX	-	-	3.1	1	2016	Fluorochemical facility
The PFOA substitute GenX detected in the environment near a fluoropolymer manufacturing plant in the Netherlands	Rotterdam, Netherlands	Groundwater	GenX	-	-	5.9	1	2017	Fluorochemical facility
The PFOA substitute GenX detected in the environment near a fluoropolymer manufacturing plant in the Netherlands	Spijkensisse, Netherlands	Groundwater	GenX	-	-	5.9	1	2018	Fluorochemical facility
The PFOA substitute GenX detected in the environment near a fluoropolymer manufacturing plant in the Netherlands	Goedereede, Netherlands	Groundwater	GenX	-	-	1.8	1	2019	Fluorochemical facility
The PFOA substitute GenX detected in the environment near a fluoropolymer manufacturing plant in the Netherlands	Alblasserdam, Netherlands	Groundwater	GenX	-	-	8	1	2020	Fluorochemical facility
The PFOA substitute GenX detected in the environment near a fluoropolymer manufacturing plant in the Netherlands	Gouda, Netherlands	Groundwater	GenX	-	-	1.4	1	2021	Fluorochemical facility
First report on the sources, vertical distribution and human health risks of legacy and novel per- and polyfluoroalkyl substances in groundwater from the Loess Plateau, China	Loess Plateau, China	Groundwater	GenX	-	2.03	-	-	2019	-
Emerging poly- and perfluoroalkyl substances in water and sediment from Qiantang River-Hangzhou Bay	Hangzhou, China	Groundwater	GenX	-	-	0.06	-	2016	-
Emerging per- and polyfluoroalkyl substances (PFASs) in surface water and sediment of the North and Baltic Seas	German	Surface Water	GenX	0.92	2.5	1.6	28	2022	Fluorochemical facility
Emerging per- and polyfluoroalkyl substances (PFASs) in surface water and sediment of the North and Baltic Seas	Elbe River, German	Surface Water	GenX	0.07	1.5	0.4	17	2023	Fluorochemical facility
Emerging per- and polyfluoroalkyl substances (PFASs) in surface water and sediment of the North and Baltic Seas	Oder Lagoon, German	Surface Water	GenX	0.028	0.037	0.034	3	2024	Fluorochemical facility

Evidence of Air Dispersion: HFPO-DA and PFOA in Ohio and West Virginia Surface Water and Soil near a Fluoropolymer Production Facility	Ohio River, West Virginia, US	Surface Water	GenX	-	-	71.2	1	2016	Fluorochemical facility
Evidence of Air Dispersion: HFPO-DA and PFOA in Ohio and West Virginia Surface Water and Soil near a Fluoropolymer Production Facility	Ohio River, West Virginia, US	Surface Water	GenX	-	-	59.4	1	2016	Fluorochemical facility
Evidence of Air Dispersion: HFPO-DA and PFOA in Ohio and West Virginia Surface Water and Soil near a Fluoropolymer Production	Ohio River, West Virginia, US	Surface Water	GenX	-	-	10.9	1	2016	Fluorochemical facility
Evidence of Air Dispersion: HFPO-DA and PFOA in Ohio and West Virginia Surface Water and Soil near a Fluoropolymer Production	Ohio River, West Virginia, US	Surface Water	GenX	-	-	10	1	2016	Fluorochemical facility
Evidence of Air Dispersion: HFPO-DA and PFOA in Ohio and West Virginia Surface Water and Soil near a Fluoropolymer Production	Ohio River, West Virginia, US	Surface Water	GenX	-	-	19.1	1	2016	Fluorochemical facility
Evidence of Air Dispersion: HFPO-DA and PFOA in Ohio and West Virginia Surface Water and Soil near a Fluoropolymer Production	Ohio River, West Virginia, US	Surface Water	GenX	-	-	22.7	1	2016	Fluorochemical facility
Evidence of Air Dispersion: HFPO-DA and PFOA in Ohio and West Virginia Surface Water and Soil near a Fluoropolymer Production	Ohio River, West Virginia, US	Surface Water	GenX	-	-	39.2	1	2016	Fluorochemical facility
Evidence of Air Dispersion: HFPO-DA and PFOA in Ohio and West Virginia Surface Water and Soil near a Fluoropolymer Production	West Fork, West Virginia, US	Surface Water	GenX	-	-	49.1	1	2016	Fluorochemical facility
Evidence of Air Dispersion: HFPO-DA and PFOA in Ohio and West Virginia Surface Water and Soil near a Fluoropolymer Production	West Virginia, US	Surface Water	GenX	-	-	53.1	1	2016	Fluorochemical facility
Evidence of Air Dispersion: HFPO-DA and PFOA in Ohio and West Virginia Surface Water and Soil near a Fluoropolymer Production	West Virginia, US	Surface Water	GenX	-	-	36.5	1	2016	Fluorochemical facility
Evidence of Air Dispersion: HFPO-DA and PFOA in Ohio and West Virginia Surface Water and Soil near a Fluoropolymer Production	West Virginia, US	Surface Water	GenX	-	-	60.8	1	2016	Fluorochemical facility
Evidence of Air Dispersion: HFPO-DA and PFOA in Ohio and West Virginia Surface Water and Soil near a Fluoropolymer Production	West Virginia, US	Surface Water	GenX	-	-	71.8	1	2016	Fluorochemical facility
Evidence of Air Dispersion: HFPO-DA and PFOA in Ohio and West Virginia Surface Water and Soil near a Fluoropolymer Production	Long Brook, West Virginia, US	Surface Water	GenX	-	-	84.3	1	2016	Fluorochemical facility

Evidence of Air Dispersion: HFPO–DA and PFOA in Ohio and West Virginia Surface Water and Soil near a Fluoropolymer Production	West Virginia, US	Surface Water	GenX	-	-	86.2	1	2016	Fluorochemical facility
Evidence of Air Dispersion: HFPO–DA and PFOA in Ohio and West Virginia Surface Water and Soil near a Fluoropolymer Production	West Virginia, US	Surface Water	GenX	-	-	41.5	1	2016	Fluorochemical facility
Evidence of Air Dispersion: HFPO–DA and PFOA in Ohio and West Virginia Surface Water and Soil near a Fluoropolymer Production	Veto Lake, West Virginia, US	Surface Water	GenX	-	-	52.6	1	2016	Fluorochemical facility
Evidence of Air Dispersion: HFPO–DA and PFOA in Ohio and West Virginia Surface Water and Soil near a Fluoropolymer Production	West Virginia, US	Surface Water	GenX	-	-	70	1	2016	Fluorochemical facility
Evidence of Air Dispersion: HFPO–DA and PFOA in Ohio and West Virginia Surface Water and Soil near a Fluoropolymer Production	West Virginia, US	Surface Water	GenX	-	-	115	1	2016	Fluorochemical facility
Evidence of Air Dispersion: HFPO–DA and PFOA in Ohio and West Virginia Surface Water and Soil near a Fluoropolymer Production	Davis Creek, West Virginia, US	Surface Water	GenX	-	-	227	1	2016	Fluorochemical facility
Evidence of Air Dispersion: HFPO–DA and PFOA in Ohio and West Virginia Surface Water and Soil near a Fluoropolymer Production	West Virginia, US	Surface Water	GenX	-	-	88.5	1	2016	Fluorochemical facility
Evidence of Air Dispersion: HFPO–DA and PFOA in Ohio and West Virginia Surface Water and Soil near a Fluoropolymer Production	West Virginia, US	Surface Water	GenX	-	-	56.8	1	2016	Fluorochemical facility
Evidence of Air Dispersion: HFPO–DA and PFOA in Ohio and West Virginia Surface Water and Soil near a Fluoropolymer Production	West Virginia, US	Surface Water	GenX	-	-	37.4	1	2016	Fluorochemical facility
Evidence of Air Dispersion: HFPO–DA and PFOA in Ohio and West Virginia Surface Water and Soil near a Fluoropolymer Production	West Virginia, US	Surface Water	GenX	-	-	44.2	1	2016	Fluorochemical facility
Evidence of Air Dispersion: HFPO–DA and PFOA in Ohio and West Virginia Surface Water and Soil near a Fluoropolymer Production	West Virginia, US	Surface Water	GenX	-	-	24.8	1	2016	Fluorochemical facility
Evidence of Air Dispersion: HFPO–DA and PFOA in Ohio and West Virginia Surface Water and Soil near a Fluoropolymer Production	Browns Run, West Virginia, US	Surface Water	GenX	-	-	30	1	2016	Fluorochemical facility
Worldwide Distribution of Novel Perfluoroether Carboxylic and Sulfonic Acids in Surface Water	Yangtze River, China	Surface Water	GenX	-	1.54	0.73	35	2018	-

Worldwide Distribution of Novel Perfluoroether Carboxylic and Sulfonic Acids in Surface Water	Yellow River, China	Surface Water	GenX	1.74	-	1.01	15	2018	-
Worldwide Distribution of Novel Perfluoroether Carboxylic and Sulfonic Acids in Surface Water	Pearl River, China	Surface Water	GenX	0.21	10.3	1.51	13	2018	-
Worldwide Distribution of Novel Perfluoroether Carboxylic and Sulfonic Acids in Surface Water	Liao River, China	Surface Water	GenX	0.62	4.51	1.44	6	2018	-
Worldwide Distribution of Novel Perfluoroether Carboxylic and Sulfonic Acids in Surface Water	Huai River, China	Surface Water	GenX	0.83	3.62	1.66	9	2018	-
Worldwide Distribution of Novel Perfluoroether Carboxylic and Sulfonic Acids in Surface Water	Chao river, China	Surface Water	GenX	0.93	3.32	1.92	13	2018	-
Worldwide Distribution of Novel Perfluoroether Carboxylic and Sulfonic Acids in Surface Water	Tai Lake, China	Surface Water	GenX	0.38	143.7	14	15	2018	-
Worldwide Distribution of Novel Perfluoroether Carboxylic and Sulfonic Acids in Surface Water	Thames River, England	Surface Water	GenX	0.7	1.58	1.12	6	2018	-
Worldwide Distribution of Novel Perfluoroether Carboxylic and Sulfonic Acids in Surface Water	Rhine River, Europe	Surface Water	GenX	0.59	1.98	0.99	20	2018	-
Worldwide Distribution of Novel Perfluoroether Carboxylic and Sulfonic Acids in Surface Water	Delaware River, US	Surface Water	GenX	0.78	8.75	3.32	12	2018	-
Worldwide Distribution of Novel Perfluoroether Carboxylic and Sulfonic Acids in Surface Water	Malaren River, England	Surface Water	GenX	0.88	2.68	1.47	10	2018	-
Worldwide Distribution of Novel Perfluoroether Carboxylic and Sulfonic Acids in Surface Water	Han River, Korea	Surface Water	GenX	0.78	2.49	1.38	6	2018	-
Presence of Emerging Per- and Polyfluoroalkyl Substances (PFASs) in River and Drinking Water near a Fluorochemical Production Plant in the Netherlands	Netherlands	Surface Water	GenX	1.7	812	-	18	2016	Chemical manufacturing facility
Spatiotemporal distribution, partitioning behavior and flux of per- and polyfluoroalkyl substances in surface water and sediment from Poyang Lake, China	Poyang Lake, China	Surface Water	GenX	0.29	5.7	0.55	-	2019	Fluorochemical facility, fire station, and metal plating site
Perfluoroalkyl substances in the Lingang hybrid constructed wetland, Tianjin, China: occurrence, distribution characteristics, and ecological risks	Tianjin, China	Surface Water	GenX	-	-	1.85	-	2019	-